Functional analyses of host factors involved in filovirus infection

（フィロウイルスの感染に関与する
宿主因子の機能解析）

KONDOH Tatsunari

Contents

Abbreviations

ANOVA	Analysis of variance
BDBV	Bundibugyo virus
BOMV	Bombali virus
BSA	Bovine serum albumin
BSL	Biosafety level
CARD	Caspase activation and recruitment domain
CBP	Central basic patch
CHAPS	3-(3-cholamidepropyl) dimethylammonio-1-propanesulphonate
cl.19	Vero E6/NPC1-KO cl.19
cDNA	Complementary DNA
cRNA	Complementary RNA
CZC	Research center for zoonosis control
DAPI	4',6-diamidino-2-phenylindole, dihydrochloride
dGP	Digested GP
DMEM	Dulbecco's modified Eagle's medium
dpi.	Days post infection
dsRNA	Double-stranded RNA
EBLN	Endogenous bornavirus-like nucleoprotein element
EBOV	Ebola virus
EDTA	Ethylenediaminetetraacetic acid
EFL	Endogenous filovirus-like element
EFL35	Filovirus VP35-like element
EFL35p	Putative protein derived from EFL35
EFLN	Filovirus NP-like element
ELISA	Enzyme-linked immunosorbent assay
EM	Electron microscopy
EMEM	Eagle's minimal essential medium
ERV	Endogenous retrovirus
FBP	First basic patch
FCS	Fetal calf serum
FFU	Focus-forming unit
GFP	Green fluorescent protein
GP	Glycoprotein
gRNA	Guide RNA

HA-mlEFL35p	HA-tagged mlEFL35p
HA-RVP35	HA-tagged RESTV VP35
HA-ZVP35	HA-tagged EBOV VP35
HEK293	Human embryonic kidney 293
HEK293T	Human embryonic kidney 293T
HIV-1	Human immunodeficiency virus type 1
HRP	Horseradish peroxidase
HU	Hokkaido University
IAV	Influenza A virus
IBC	Institutional Biosafety Committee
IFN	Interferon
Ig	Immunoglobulin
IID	IFN inhibitory domain
IKKε	Inhibitor of κB kinase epsilon
IP	Immunoprecipitation
IPS-1	IFN-β promoter stimulator 1
IRF	Interferon regulatory factor
IU	Infectious unit
KO	Knockout
L	RNA-dependent RNA polymerase
LC8	8-kDa cytoplasmic dynein light chain
LLOV	Lloviu virus
Luc	Luciferase
MARV	Marburg virus
me	*Macropus eugenii*
ml	*Myotis lucifugus*
MOI	Multiplicity of infection
MSRV	Multiple sclerosis-associated retrovirus
NCBI	National Center for Biotechnology Information
NIAID	National Institute of Allergy and Infectious disease
NIH	National Institute of Health
NP	Nucleoprotein
NPBP	NP-binding peptide
NPC1	Niemann-Pick C1
OD450	Optical density at 450 nm
ORF	Open reading frame

PACT	PKR activator
PAGE	Polyacrylamide gel electrophoresis
PAM	Proto-spacer Adjacent Motif
PBS	Phosphate-buffered saline
PBST	PBS containing 0.05% (vol/vol) Tween 20
PCR	Polymerase chain reaction
PDB	Protein data bank
PFU	Plaque-forming unit
PKR	Protein kinase RNA-activated
Plat-GP	Platinum-GP
PVDF	Polyvinylidene fluoride
RAVV	Ravn virus
RESTV	Reston virus
RIG-I	Retinoic acid-inducible gene-I
RML	Rocky Mountain Laboratories
rVSV	Replication-competent recombinant VSV
SDS	Sodium dodecyl sulfate
SNP	Single nucleotide polymorphism
SOP	Standard opening procedure
SUDV	Sudan virus
TAFV	Tai Forest virus
TBK1	TANK-binding kinase 1
$TCID_{50}$	Tissue culture infectious dose for 50%
TK	Thymidine kinase
ts	Tarsier
TSD	Target site duplication
VP	Viral protein
vRNA	Viral RNA
VSV	Vesicular stomatitis virus
293T-NPC1	HEK293T NPC1
2-ME	2-Mercaptoethanol

Preface

Filoviruses, which belong to the family *Filoviridae*, are filamentous, enveloped, and non-segmented negative-strand RNA viruses. Ebolaviruses and marburgviruses are members of this virus family and cause severe hemorrhagic fever in humans and nonhuman primates. *Filoviridae* consists of three genera, encompassing seven species (five species in the genus *Ebolavirus*, and one species each in the genera *Marburgvirus* and *Cuevavairus*)[45]. Currently, eight distinct viruses are assigned to these seven species: Ebola virus (EBOV), Bundibugyo virus (BDBV), Tai Forest virus (TAFV), Sudan virus (SUDV), and Reston virus (RESTV) in the genus *Ebolavirus*; Marburg virus (MARV) and Ravn virus (RAVV) in the genus *Marburgvirus*; and Lloviu virus (LLOV) in the genus *Cuevavirus*. In addition, a new filovirus, Bombali virus (BOMV) has been recently discovered from free-tailed bats in Sierra Leone[27]. BOMV will be assigned to the genus *Ebolavirus*. RESTV has never caused lethal infection in humans[8], and the biological properties of LLOV and BOMV have not been characterized, since the infectious forms of these viruses have not been yet isolated[27,42,69]. Filoviruses are considered a significant public health concern because ebolaviruses and marburgviruses have continuously produced sporadic outbreaks with increased frequencies in Central and West Africa[13,83].

A filovirus particle consists of at least seven structural proteins: envelope glycoprotein (GP), nucleoprotein (NP), viral protein (VP) 40, VP35, VP30, VP24, and RNA-dependent RNA polymerase (L) (Fig. 1A). GP is the only viral surface protein of filoviruses and mediates viral entry into cells[90] (Fig. 1B). During the entry process, GP interacts with multiple host factors (e.g., attachment factor and fusion receptor). Infection is initiated by the binding of the virus to attachment factors such as C-type lectins[35,88], and virus particles are then internalized into the host cells via macropinocytosis[67,81]. Virus

A

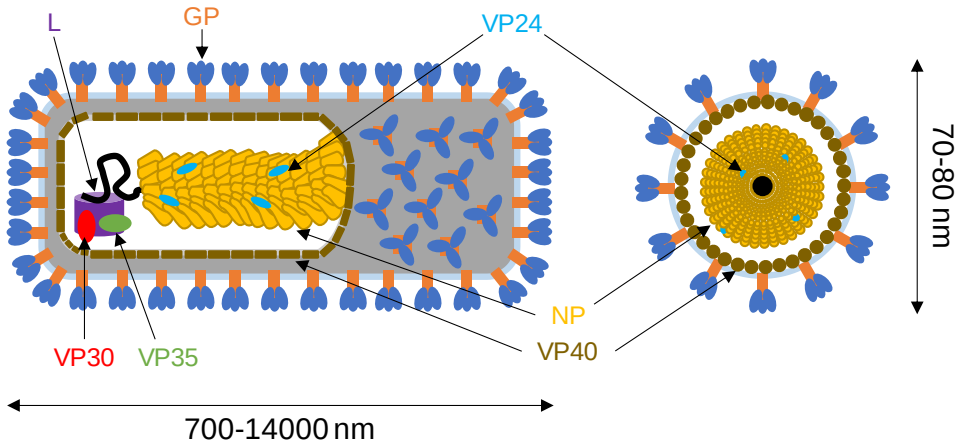

Fig. 1. Structure of a filovirus particle and the model of GP-mediated viral entry into cells. (A) Schematic diagrams of a filovirus particle. (B) Current model of filovirus entry into cells. Glycan structures on the mucin-like region on the GPs bind to attachment factors such as C-type lectin, and virus particles are then internalized into the host cells via macropinocytosis. A viral particle is delivered to the late endosome. A low pH leads to the proteolytic processing of the GPs through cysteine-proteases (e.g., cathepsins B and L). The digested GP exposes its receptor-binding region and interacts with Niemann-Pick C1 (NPC1), a ubiquitous host endosomal cholesterol transporter. NPC1 contains 13 transmembrane helices, 3 large luminal hydrophilic loops, and a cytoplasmic tail[16]. Membrane fusion between the viral envelope and host cell endosomal membrane occurs and the ribonucleoprotein complex is released into the cytoplasm.

B

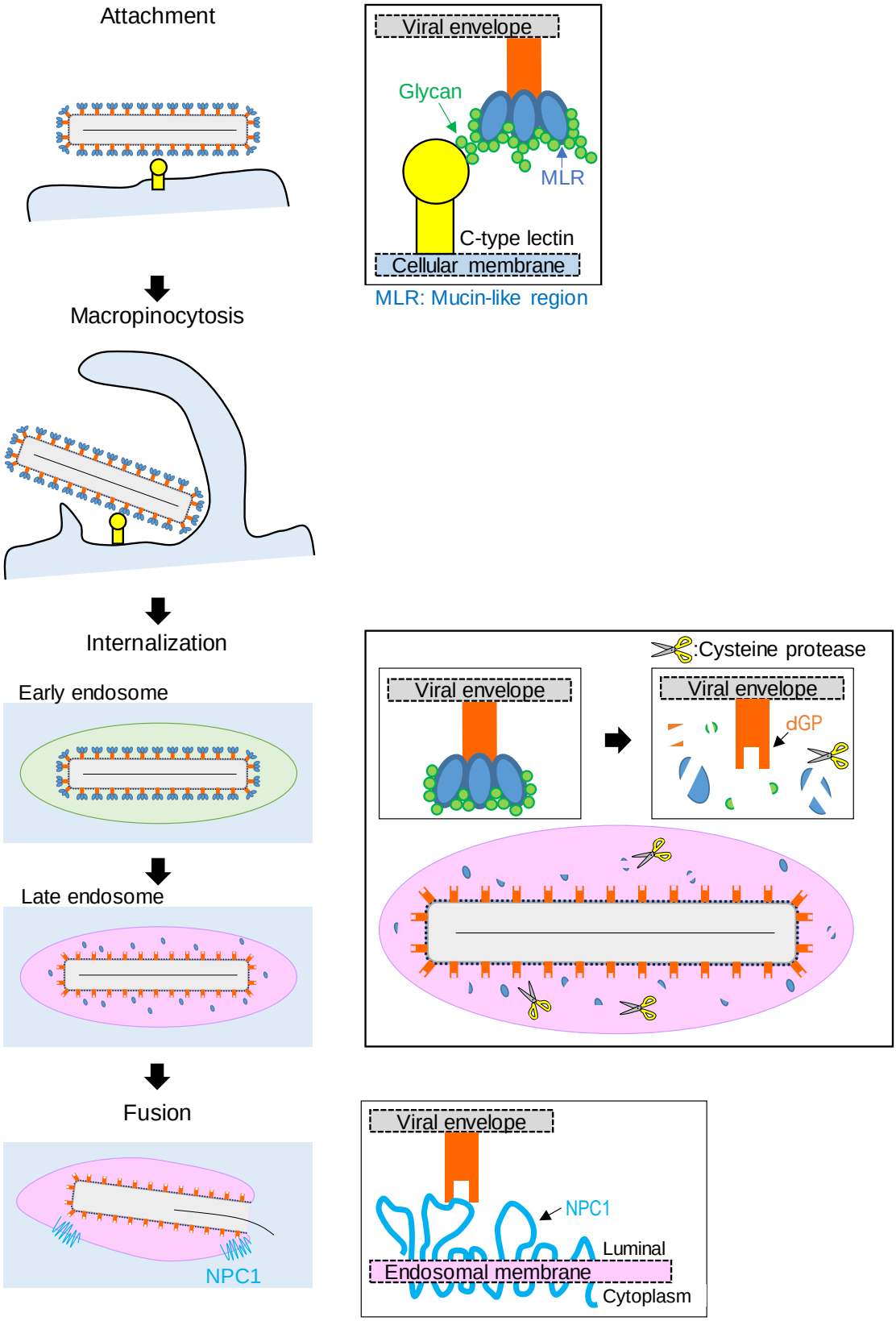
Attachment
Viral envelope
Glycan
MLR
C-type lectin
Cellular membrane
MLR: Mucin-like region
Macropinocytosis
Internalization
:Cysteine protease
Viral envelope
Viral envelope
dGP
Early endosome
Late endosome
Fusion
NPC1
Viral envelope
NPC1
Luminal
Endosomal membrane
Cytoplasm

particles are delivered to the late endosome. A low late-endosomal pH leads to the cysteine protease-mediated proteolysis of GP[12,62]. This digested GP (dGP) can then interact with the host endosomal fusion receptor NPC1 allowing fusion between the viral envelope and the host endosomal membrane[10,15,61]. Thus, NPC1 represents a major determinant of cell susceptibility to filovirus infection[68,70].

Following GP-mediated membrane fusion, the ribonucleoprotein complex consisting of NP, VP35, VP30, VP24, and L is released into the cytoplasm of the cells. Each filovirus gene is transcribed into mRNA by VP35 and L, and the viral mRNAs are then translated into viral proteins by the host cell machinery. Filovirus VP35 is well documented as an antagonist of interferon (IFN) and a polymerase cofactor for transcription and replication of the viral genome[5,64]. VP35 inhibits retinoic acid-inducible gene-I (RIG-I)-mediated host innate immunity (Fig. 2A) and also drives the synthesis of full-length complementary and antigenomic RNAs in cooperation with NP, VP30, and L (Fig. 2B). Interestingly, a nucleotide sequence that is closely related to the filovirus VP35 gene was recently discovered in the genome of some species of bats[6]. This sequence is called an endogenous filovirus VP35-like element (EFL35). Although the biological significance of EFL35 is largely unknown, it is speculated that the presence of EFL35 in host genomes may be correlated with cellular susceptibility to filovirus infection[6,94].

Filoviruses infect a variety of cell types *in vitro*[11,20,30,39,59,90], and several cellular factors are shown to be involved in filovirus infection[38,88]. However, the details of the mechanisms underlying the cell tropism and pathogenicity of filoviruses have not yet been fully elucidated. To obtain a better understanding of filovirus infection, I focused on filoviral entry, replication, and immune evasion mechanisms. In chapter I, I have investigated the relationship between single-nucleotide polymorphisms (SNPs) in human

NPC1 and cell tropism of filoviruses. In chapter II, I have analyzed and discussed the potential role of the putative protein derived from EFL35 *in vitro*.

A

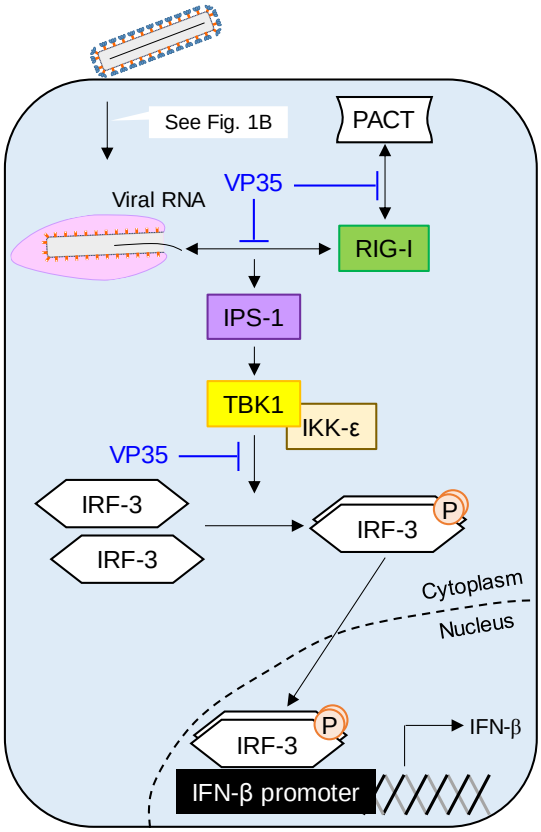

Fig. 2. Biological function of VP35. (A) Filovirus VP35 binds to RNA and sequesters viral RNA after its recognition by RIG-I. EBOV VP35 inhibits IFN-β production by interacting with the IRF-3 kinases IKK-ε and TBK-1. Ebolavirus VP35 also interacts with the RIG-I activator PACT and interferes with RIG-I activation. (B) VP35 also plays an important role in viral transcription /replication. Transcription results in the synthesis of seven monocistronic mRNAs that are capped and polyadenylated. Replication starts with the synthesis of a full-length positive-sense complementary RNA (cRNA). The cRNA serves as a template for the generation of negative-sense viral RNA (vRNA).

B

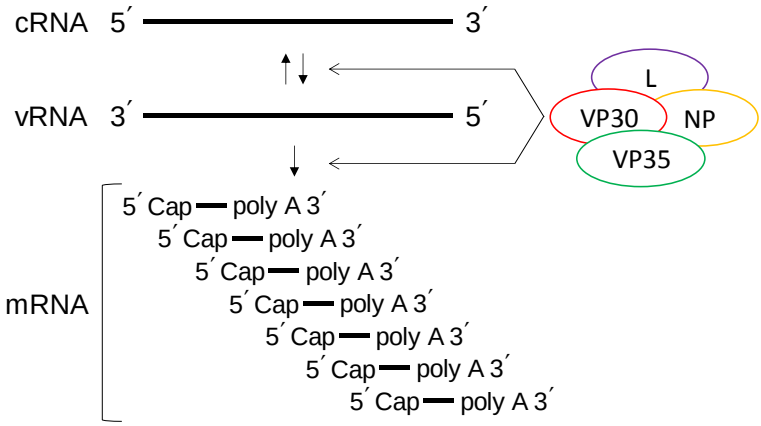

Chapter I:
Single-nucleotide polymorphisms in human NPC1 affecting filovirus entry into cells

Introduction

The recently published co-structures of EBOV dGP in complex with NPC1 revealed that two surface-exposed loops on NPC1 mediate its interaction with dGP[28,97]. Biochemical analysis of purified NPC1 and dGP has further shown that amino acid substitutions in these two loops (e.g., P424A, F503G, and F504G) reduce its binding to dGP[97]. This finding led me to hypothesize that SNPs in human NPC1 might influence host susceptibility to filovirus infection. Mutations tested in previous studies[68,70,97] were not linked to human NPC1 SNPs and are unregistered in the SNP database (https://www.ncbi.nlm.nih.gov/snp/). Thus, it remains unknown whether naturally occurring SNPs found in human NPC1 can affect the efficiency of filovirus infection.

Using a structure-guided approach to the SNP database, I identified 10 missense SNPs in the GP-interacting loop regions of NPC1. To investigate the potential effects of these substitutions on filovirus infection *in vitro*, I generated an NPC1 knockout Vero E6 cell line and established stable cell lines expressing the NPC1 SNP mutants. Cell susceptibility was examined using vesicular stomatitis virus (VSV) pseudotyped with filovirus GPs[89,90], as well as a replication-competent EBOV expressing the green fluorescent protein (GFP)[21]. Here, I report human NPC1 SNPs that influence the susceptibility of cells to filovirus entry and infection.

Materials and Methods

Viruses

VSV containing the GFP gene instead of the receptor-binding VSV-G protein gene (VSVΔG) and pseudotyped viruses with GPs of EBOV (Mayinga), BDBV (Butalya), TAFV (Pauléoula), SUDV (Boniface), RESTV (Pennsylvania), MARV (Angola), RAVV (Kitum Cave), and LLOV (Asturias), designated by VSVΔG-EBOV, -BDBV, -TAFV, -SUDV, -RESTV, -MARV, -RAVV, and -LLOV, respectively, were generated as described previously[25,90]. Infectious units (IUs) of these pseudotyped VSVs were determined in Vero E6 cells as previously described[59,90]. Replication-competent recombinant VSVs (rVSV-EBOV [Mayinga] and rVSV-MARV [Angola]) were generated as described previously[89]. rVSV-EBOV, rVSV-MARV, and recombinant EBOV expressing GFP (EBOV-GFP)[21] were propagated in Vero E6 cells and stored at -80°C. Infectivity of rVSV-EBOV, rVSV-MARV, and EBOV-GFP in each cell line was determined by plaque- and focus-forming assays, as described previously[22,37]. Relative infectivity in each cell line was calculated by setting the IU, plaque-forming unit (PFU), or focus-forming unit (FFU) values of the NPC1 knockout Vero E6 cells expressing human NPC1 to 100%.

Biosafety

All work using infectious EBOV-GFP was performed in the biosafety level-4 (BSL-4) laboratory at the Integrated Research Facility of the Rocky Mountain Laboratories (RML), Division of Intramural Research, National Institute of Allergy and Infectious Diseases (NIAID), National Institutes of Health (NIH), Hamilton, Montana, USA. All standard operating procedures (SOPs) were approved by the Institutional Biosafety Committee (IBC) in the NIH. All works using pseudotyped VSVs with filovirus

GPs were performed in the BSL-2 and BSL-3 laboratories in the Research Center for Zoonosis Control (CZC), Hokkaido University (HU).

Cell lines

Vero E6 cells (ATCC® CRL-1586™), NPC1 knockout Vero E6 (Vero E6/NPC1-KO), and HEK293T-derived Platinum-GP (Plat-GP) cells[44] (Cell Biolabs) were grown in Dulbecco's modified Eagle's medium (DMEM, Sigma) supplemented with 10% fetal calf serum (FCS).

Titration of VSV pseudotyped with filovirus GPs

Confluent monolayers of each cell line grown in 96-well plates were infected with VSVΔG-EBOV, VSVΔG-BDBV, VSVΔG-TAFV, VSVΔG-SUDV, VSVΔG-RESTV, VSVΔG-MARV, VSVΔG-RAVV, and VSVΔG-LLOV. Twenty hours later, the IUs in each cell line were determined by counting the number of GFP-expressing cells with an IN Cell Analyzer 2000 (GE Healthcare)[59]. Relative infectivity in each cell line was calculated by setting the IU value given by Vero E6/NPC1-KO cells expressing human NPC1 (approximately 1000-3000 IU/well for each assay) to 100%.

Viral plaque assay

Infectivity of rVSV-EBOV and rVSV-MARV in each cell line was determined by plaque-forming assays as described previously[37]. Briefly, rVSV-EBOV and rVSV-MARV (multiplicity of infection, MOI = 0.0005 in Vero E6 cells) were inoculated into Vero E6 cells grown in six-well tissue culture plates. After adsorption for one hour, the inoculum was removed, and the cells were overlaid with Eagle's minimal essential medium (EMEM) containing 1.0% Bacto Agar (BD) and then incubated for 3 days at

37°C. Cells were stained with 0.5 % crystal violet in 10% formalin and the PFUs in each cell line were determined by counting the number of all visible plaques per well (i.e., 50-100 plaques for each assay). Plaque sizes were measured using the Image-J software (https://imagej.nih.gov).

Focus-forming assay

Infectivity of EBOV-GFP in each cell line was determined by focus-forming assays. EBOV-GFP (MOI = 0.002 in Vero E6 cells) were inoculated into confluent monolayers of Vero E6 cells grown in 96-well tissue culture plates. After adsorption for one hour, the inoculum was replaced with EMEM containing 1.2% carboxymethyl cellulose[22]. After incubation for three days at 37°C, the cells were fixed and the GFP foci in each cell line were counted under a fluorescence microscope. Sizes of the foci were measured using the Image-J software (https://imagej.nih.gov).

Cloning of the NPC1 gene into plasmids

The coding region of the HEK293T NPC1 (293T-NPC1) gene was polymerase chain reaction (PCR) amplified from cDNA prepared from total RNA extracted from HEK293T cells, according to a previous study[46]. The PCR product was cloned into a murine leukemia virus-based retroviral vector, pMXs-puro[44]. As shown in Table 1, a total of 10 SNPs were found in the two loops (i.e., two loop structures at amino acid positions 419-428 and 500-508). All NPC1s were produced by site-directed mutagenesis using a KOD-Plus-Neo polymerase (TOYOBO) with primers containing the desired nucleotide substitutions (Table 2). All mutations were confirmed by DNA sequencing.

Establishment of the Vero E6/NPC1-KO cell line

Vero E6/NPC1-KO cells were generated by previously described methods[52,99] with a few modifications. We found a candidate guide RNA (gRNA) target sequence in the genomic region of Vero E6 NPC1 and the designed oligonucleotides (CRISPR-VeroNPC1-F1: 5′-TAATACGACTCACTATAGCTGCTACTGTGTCCGGCGC-3□ and CRISPR-VeroNPC1-R1: 5′-TTCTAGCTCTAAAACGCGCCGGACACAGTAGCAG-3′) by using the CRISPRdirect web tool (https://crispr.dbcls.jp/)[66]. Synthesis of a gRNA template, *in vitro* transcription of gRNA, and purification of gRNA products were performed using the GeneArt precision gRNA synthesis kit (Invitrogen) according to the manufacturer's instructions. Vero E6 cells were transfected with the gRNA products and the Platinum Cas9 nuclease (Invitrogen) mixture using Lipofectamine CRISPRMAX Cas9 Transfection Reagent (Invitrogen) according to the manufacturer's instructions, followed by incubation for three days at 37°C. By means of a genomic cleavage detection assay with a specific primer set (VeroNPC1-367F: 5′-CTGAGGAGAAGGGCAAAG-3′ and VeroNPC1-846R: 5′-CATCGCTAGACCAACTTCC-3′) using a GeneArt Genomic Cleavage Detection Kit (Invitrogen), I confirmed the presence of a cleaved DNA product comprising 426 base pairs resulting from the introduction of the gRNA into the cells. I retreated the transfected Vero E6 cells with Cas9 nuclease mixture to generate double knockout cells. For clonal isolation, the transfected cell suspension (5 cells/ml) was seeded onto 96-well plates precoated with poly D-lysine (Nunc). After clonal expansion for three weeks, I obtained 97 clones. Cells from each well were harvested, followed by Western blotting to confirm that there was no expression of NPC1. Of the 97 clones examined, I selected two clones (Vero E6/NPC1-KO cl. 19 and cl. 89), and used Vero E6/NPC1-KO cl. 19 (cl. 19) for the following experiments.

Table 1. SNPs identified in this study.

rsID	Codons	Position in the protein	Amino Acid	Symbol
rs772847092	ATT/TTT	419	I/F	I419F
rs772847092	ATT/GTT	419	I/V	I419V
rs77815278	TAC/TCC	420	Y/S	Y420S
rs771644708	TAC/CAC	420	Y/H	Y420H
rs143797098	CCT/GCT	424	P/A	P424A
rs140149624	TCG/TTG	425	S/L	S425L
rs749078710	GCT/ACT	427	A/T	A427T
rs748246747	GGG/GAG	500	G/E	G500E
rs191537721	GAC/GAG	502	D/E	D502E
rs756587493	GAT/AAT	508	D/N	D508N

Table 2. Oligonucleotide sequences used for mutagenesis

Primer name	Sequences
293T-NPC1-I419F-F	5'-CTCTCACTGACAAACACTTTTACCAGCCATACCCT-3'
293T-NPC1-I419F-R	5'-AGGGTATGGCTGGTAAAAGTGTTTGTCAGTGAGAG-3'
293T-NPC1-I419V-F	5'-AGGGTATGGCTGGTAAACGTGTTTGTCAGTGAGAG-3'
293T-NPC1-I419V-R	5'-CTCTCACTGACAAACACGTTTACCAGCCATACCCT-3'
293T-NPC1-Y420H-F	5'-GGTATGGCTGGTGAATGTGTTTGTCAGTGAGAGGGG-3'
293T-NPC1-Y420H-R	5'-CCCCTCTCACTGACAAACACATTCACCAGCCATACC-3'
293T-NPC1-Y420S-F	5'-GGGTATGGCTGGCTAATGTGTTTGTCAGTGAGAGGGG-3'
293T-NPC1-Y420S-R	5'-CCCCTCTCACTGACAAACACATTAGCCAGCCATACCC-3'
293T-NPC1-P424A-F	5'-AACACATTTACCAGCCATACGCCTCGGGAGCTGATGTAC-3'
293T-NPC1-P424A-R	5'-GTACATCAGCTCCCGAGGCGTATGGCTGGTAAATGTGTT-3'
293T-NPC1-S425L-F	5'-ACATTTACCAGCCATACCCTCTGGGAGCTGATGTACCC-3'
293T-NPC1-S425L-R	5'-GGGTACATCAGCTCCCAGAGGGTATGGCTGGTAAATGT-3'
293T-NPC1-A427T-F	5'-CCAAAGGGTACATCAGTTCCCGAAGGGTATGGC-3'
293T-NPC1-A427T-R	5'-GCCATACCCTTCGGGAACTGATGTACCCTTTGG-3'
293T-NPC1-G500E-F	5'-ACACAAAGAAGTCGTCCTCTTTCTTGTGGTCCAGC-3'
293T-NPC1-G500E-R	5'-GCTGGACCACAAGAAAGAGGACGACTTCTTTGTGT-3'
293T-NPC1-D502E-F	5'-CACAAGAAAGGGGACGAGTTCTTTGTGTATGCCGA-3'
293T-NPC1-D502E-R	5'-TCGGCATACACAAAGAACTCGTCCCCTTTCTTGTG-3'
293T-NPC1-D508N-F	5'-GAAAGTGCGTGTGGTAATTGGCATACACAAAGAAGTC-3'
293T-NPC1-D508N-R	5'-GACTTCTTTGTGTATGCCAATTACCACACGCACTTTC-3'

Generation of each NPC1-expressing cell line

To generate the retrovirus, Plat-GP cells were cotransfected with pMXs-puro encoding 293T-NPC1 or the cDNA of each NPC1 mutant and the expression plasmid pCAGGS[71] encoding VSV-G cDNA using the FuGENE HD transfection reagent (Promega) according to the manufacturer's recommendations. Two days later, the culture supernatants containing the retroviruses were collected, and filtered through 0.45-μm filters. The cl. 19 cells were transduced with retroviruses expressing 293T-NPC1 and its mutant genes. Cell lines stably expressing each NPC1 SNP were selected by culturing the cells in DMEM containing 10% FCS and 20 μg/ml puromycin (Sigma).

SDS-PAGE and Western blotting

Cells (2.0×10^6 cells for each cell line) were lysed with 100 μl of TNE-CHAPS buffer (10 mM Tris-HCl [pH 7.5], 140 mM NaCl, 1 mM EDTA, and 0.5% wt/vol CHAPS)[61] containing a protease inhibitor mixture (Roche). To facilitate the disruption of the cells, cell suspensions were frozen at -80°C. The samples were centrifuged at 10000 ×*g* and 4°C for 10 min. The supernatants were mixed with sodium dodecyl sulfate (SDS)-polyacrylamide gel electrophoresis (PAGE) sample buffer (Bio-Rad) with 10% 2-mercaptoethanol (2-ME) and incubated at 65°C for 15 min. The expressed proteins were separated on a SDS- polyacrylamide gel (SuperSep Ace 5-20%, Wako) and transferred onto polyvinylidene fluoride (PVDF) membranes (Merck). Phosphate-buffered saline (PBS) containing 3% (wt/vol) skim milk (BD) and PBS containing 0.05% (vol/vol) Tween 20 (PBST) were used as blocking and wash buffers, respectively. The PVDF membranes were incubated with an anti-NPC1 rabbit antibody (abcam, ab108921) that recognizes the polypeptide-containing amino acid residues from position 1250 to the C-terminus of human NPC1, and an anti-β actin mouse monoclonal antibody (abcam,

ab6276) for 60 min, washed with PBST, and then incubated with horseradish peroxidase (HRP)-conjugated goat anti-mouse IgG (Jackson ImmunoResearch, 115-035-062) and HRP-conjugated goat anti-rabbit IgG (KPL, 074-1506) for 60 min. After washing with PBST, the bound antibodies were visualized using the Immobilon Western (Millipore) system. The relative expression levels were analyzed with the Amersham Imager 600 Software (GE Healthcare).

DNA sequencing

The DNA cleavage site in the cl.19 was PCR-amplified from genomic DNA, which was extracted from cl.19 using ISOGENOME (NIPPON GENE). The following sense and antisense primers (VeroNPC1-367F: 5′-CTGAGGAGAAGGGCAAAG-3′ and VeroNPC1-846R: 5′-CATCGCTAGACCAACTTCC-3′) and KOD-Plus Neo (TOYOBO) were used for the amplification of the cleavage site. The PCR product was purified using a gel extraction kit (Promega) and was sequenced using the Big Dye V3.1 Terminator Kit (Applied Biosystems) and the 3130 Genetic Analyzer (Applied Biosystems).

Real-time PCR

To compare the transcription levels of the NPC1 genes in the stable cell lines, the copy numbers of NPC1 mRNA were analyzed with real-time PCR using the comparative CT method using Quant Studio 3 (Applied Biosystems). RNA extraction and reverse transcription from the lysates of the cultured cells was conducted using a Power SYBR® Green Cells-to-CT Kit (Applied Biosystems), and the real-time PCR mixtures were prepared using the PowerUp™ SYBR™ Green Master Mix (Applied Biosystems) and 0.4 μM of the primers (HEK293T-NPC1-2987F: 5'-TGAGATTCCTGCCCATGTTC-3'; HEK293T-NPC1-3086R: 5'-TGGCCAAGGAGGATGTTAAC-3'; hum_b-actin-270F:

5'-TTCTACAATGAGCTGCGTGTG-3'; hum_b-actin-389R: 5'-GGGGTGTTGAAGGTCTCAAA-3'). The PCR reactions were performed according to the manufacturer's instructions.

Indirect immunofluorescence assay

Cells from each cell line were seeded onto eight-well chamber slides (Watson). One day after seeding, the cells were fixed in 4% (wt/vol) paraformaldehyde for 40 min at room temperature, and permeabilized by incubation for 15 min in PBS containing 0.5% (vol/vol) Triton X-100. The cells were then incubated with PBS containing 3% (wt/vol) bovine serum albumin (BSA), followed by incubation with the anti-NPC1 mouse antibody (abcam, ab55706) and anti-LAMP1 rabbit antibody (Sigma, SAB3500285) overnight at 4°C. The cells were washed using a wash buffer (0.3% BSA, 0.1% Triton-X 100 in PBS), and then incubated with Alexa Fluor 488-conjugated goat anti-rabbit IgG (Molecular Probes, A21206) and Alexa Fluor 594-conjugated goat anti-mouse IgG (Molecular Probes, A11032) for 30 min in the dark. The nuclei were stained using 1 μg/ml 4',6-diamidino-2-phenylindole, dihydrochloride (DAPI, Molecular Probes, D1306) for 10 min in the dark. Images were acquired with a 63 × oil objective lens on a Zeiss LSM700 inverted microscope and using the ZEN 2009 software (Carl Zeiss).

Statistical analyses

All statistical analyses were performed using the R software[95]. Correlations between the transcription and expression levels of NPC1 were estimated using the rank correlation coefficient of Spearman (r_s). For the comparison of viral infectivity and plaque/focus size, the one-way ANOVA, followed by Dunnett's test and Welch's *t*-test, was used. *P*-values less than 0.05 were considered statistically significant.

Results

Structure-guided approach for identifying candidate NPC1 SNPs

Human NPC1 has at least 254 unique SNPs listed in the SNP database (https://www.ncbi.nlm.nih.gov/snp/). Of these SNPs, 222 are missense, resulting in amino acid changes, and they are widely distributed throughout the structure of NPC1 (Fig. 3A and 3B.). Using the data of the co-structure of full-length NPC1 and EBOV dGP[28], I identified 10 missense SNPs in 8 amino acid positions located in the GP-interacting loop regions of the domain C of NPC1 (Fig. 3B and 3C.).

Human NPC1 polymorphisms affecting filovirus entry into cells

I next established an NPC1 knockout Vero E6 cell line, cl.19 (Fig. 4A and 4B), and confirmed that its susceptibility to VSVΔG- EBOV, rVSV-EBOV, and EBOV-GFP was completely abolished (Fig. 4C-4E). The cl.19 cells were then transduced with a retroviral vector, resulting in eleven different cell lines stably expressing 293T-NPC1 or its SNP mutants (I419V, I419F, Y420S, Y420H, P424A, S425L, A427T, G500E, D502E, and D508N). Introducing the 293T-NPC1 gene into the knockout cells completely restored their susceptibility to filovirus entry and infection (Fig. 4C-4E), as has been shown with NPC1-deficient CHO and reptile-derived cells[10,61]. The transcription and expression levels of the transduced NPC1 genes were examined by quantitative PCR and Western blot analyses, respectively. In all the NPC1 SNP mutant cell lines, the expression levels of NPC1 were equivalent to or higher than those in the 293T-NPC1-expressing cells (Fig. 5). I also confirmed that these NPC1s were localized at the endosomal vesicles (Fig. 6). To evaluate whether these SNP substitutions affected the efficiency of viral entry, cells from each cell line were infected with replication-incompetent VSV pseudotyped

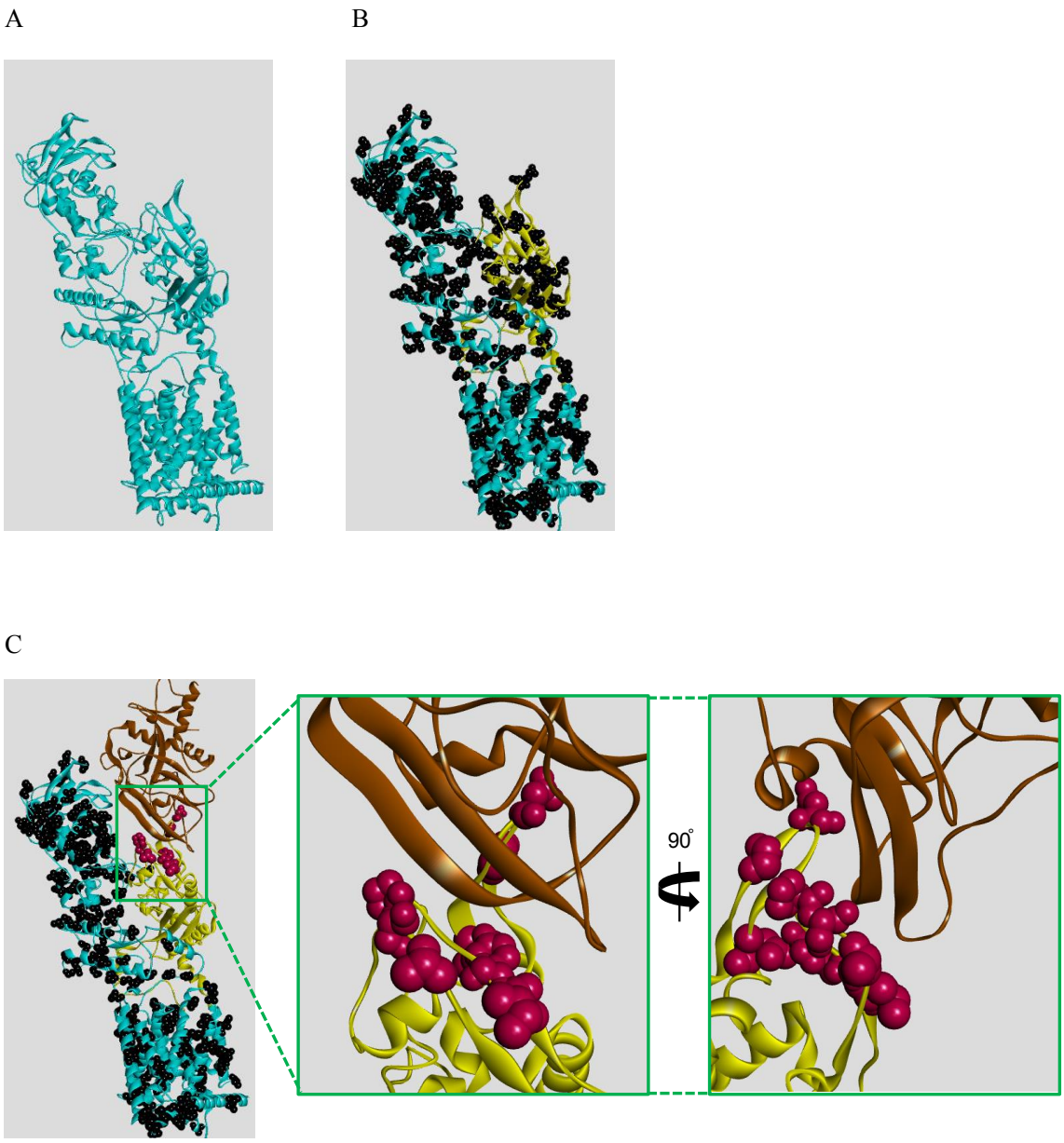

Fig. 3. Structure-guided approach to human NPC1 SNP selection. (A) Cryo-EM structure of the full-length human NPC1 is shown in light blue. (B) 222 missense SNPs on the NPC1 structure are shown in black. The domain C of NPC1 (NPC1-C) is colored in yellow. (C) The co-structure of digested EBOV GP (brown) and NPC1-C (yellow) with the amino acid positions of the SNPs shown in maroon. (A-C) All the structures in this figure have been modified from Protein Data Bank (PDB) code 5JNX using Discovery Studio (Dassault Systèmes BIOVIA).

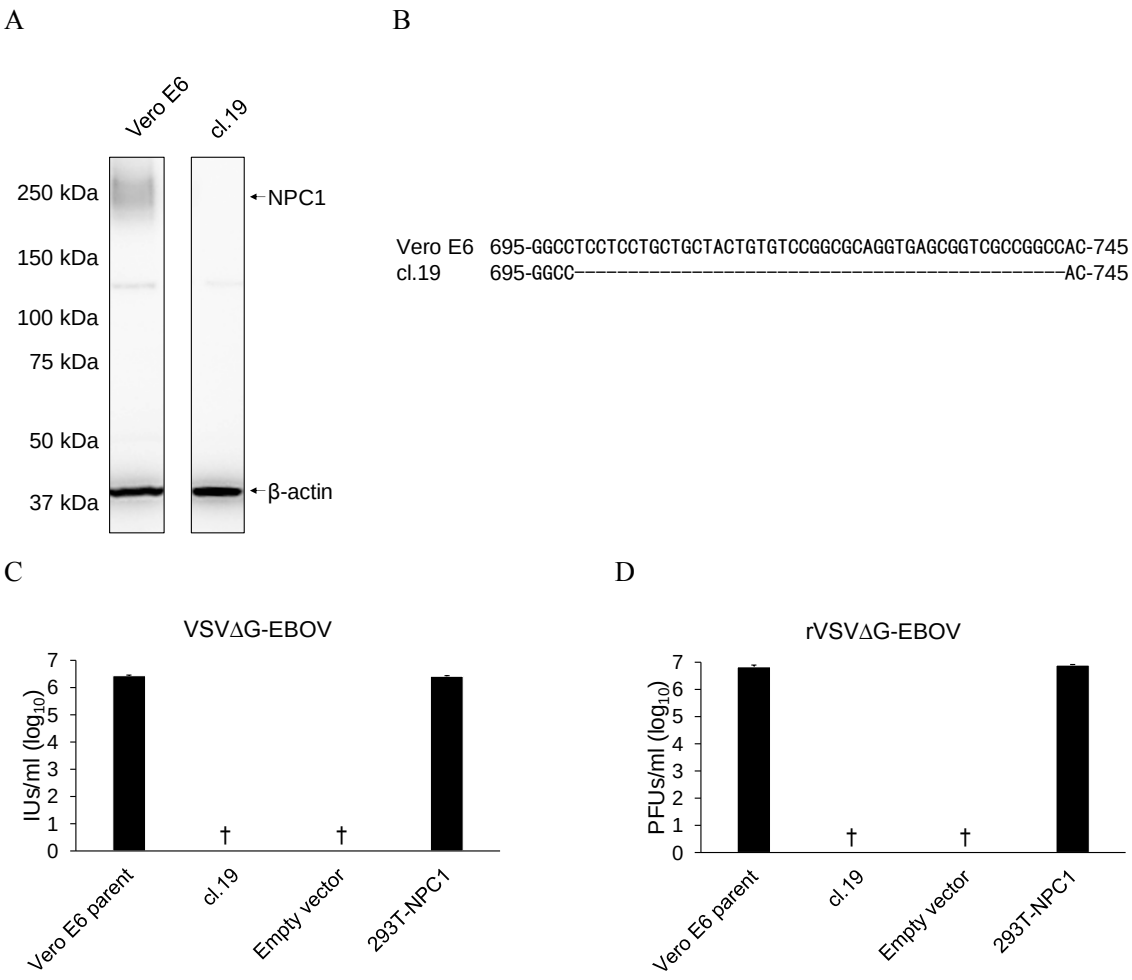

Fig. 4. Generation of Vero E6/NPC1-KO cells and their susceptibility to VSVΔG-EBOV, rVSV-EBOV, and EBOV-GFP. (A) Expression of NPC1 in the parent Vero E6 and Vero E6/NPC1-KO clone 19 (cl. 19) cells was analyzed by Western blotting. The results described here are splicing lanes from different sections of a membrane. The experiment was performed three times and representative data are shown. (B) Deletion of the desired region of the NPC1 gene in cl. 19 cells was confirmed by DNA sequencing. (C-E) Parent Vero E6, cl. 19, and cl. 19 cells transduced with an empty vector, and cl. 19 cells stably expressing 293T-NPC1 were infected with VSVΔG-EBOV (C), rVSV-EBOV (D), or EBOV-GFP (E). (C-E) The data represent the means and standard errors of triplicate assays. †: Not detected.

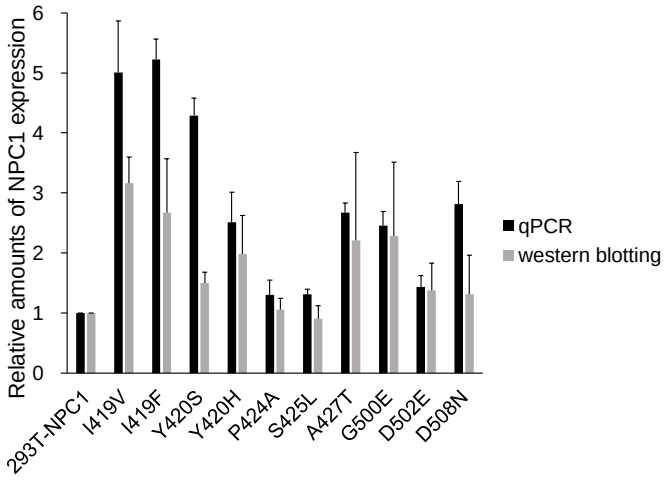

Fig. 5. Transcription and expression levels of NPC1 in each stable cell line. Transcription levels of the NPC1 mRNAs were analyzed using qPCR and Western blotting. The data represent the means and standard deviations of at least three independent experiments. The Spearman rank correlation coefficient (r_s) showed that the transcription and expression levels of NPC1 were significantly correlated ($r_s = 0.63$, *P*-value = 0.000073).

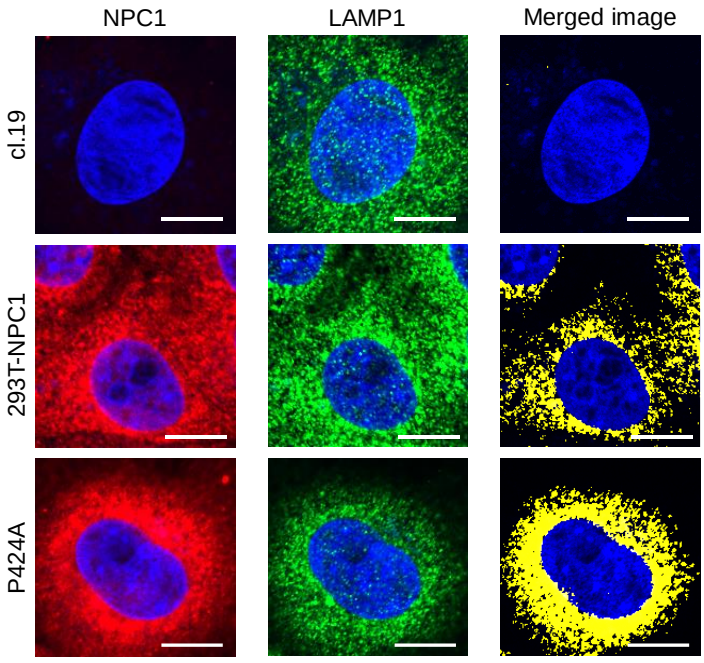

Fig. 6. Co-localization of NPC1 and LAMP1. The expression and co-localization of NPC1 and LAMP1 have been compared. Representative data (of Vero E6/NPC1-KO [cl. 19] cells, cl. 19 cells stably expressing HEK293T-NPC1 [293T-NPC1], and cl. 19 cells stably expressing P424A [P424A]) are provided here. The expression of NPC1 (red) and LAMP1 (green) are shown separately or as merged images (yellow). The scale bars represent 10 μm. The nuclei of the cells are visualized with DAPI (blue).

with filovirus GPs, and the relative IUs among the cell lines were compared (Fig. 7). I found that the P424A, S425L, D502E, and D508N substitutions in NPC1 reduced the entry of VSV pseudotyped with GPs from multiple filovirus species. The P424A and D508N substitutions significantly affected the entry of VSVΔG-EBOV, -BDBV, -TAFV, -SUDV, -RESTV, and -LLOV, but not -MARV and/or -RAVV. However, the S425L and D502E substitutions reduced the entry of VSVΔG-MARV, and some of the VSVs pseudotyped with ebolavirus GPs. The Y420S substitution only reduced the entry of VSVΔG-LLOV. It was noted that these substitutions resulted in different patterns of reduction corresponding to the filovirus genera (i.e., *Ebolavirus*, *Marburgvirus*, and *Cuevavirus*). In particular, the P424A/D508N and S425L/D502E substitutions seemed to be important for the reduced entry of VSVs pseudotyped with ebolavirus and marburgvirus GPs, respectively. In some cell lines, the infectivity of the viruses was enhanced and was correlated with relatively high expression levels of NPC1 (Fig. 5).

Reduced plaque-forming ability of rVSV-EBOV in Vero E6 cells expressing NPC1 with the P424A or D508N substitution

I then compared the plaque-forming abilities of rVSV-EBOV and rVSV-MARV using the same cell lines (Fig. 8). Although a statistically significant difference was not observed, the P424A and S425L substitutions moderately reduced the number of plaques formed by rVSV-EBOV and rVSV-MARV, respectively (Fig. 8A). As expected, the average plaque sizes of rVSV-EBOV in cells expressing NPC1 with the D508N substitution were significantly smaller than those in 293T-NPC1-expressing cells, and the P424A substitution also slightly reduced the plaque size (Fig. 8B). Consistent with the data shown in Fig. 7, rVSV-MARV formed slightly, but not significantly smaller plaques in the cell line expressing S425L NPC1 (Fig. 8B).

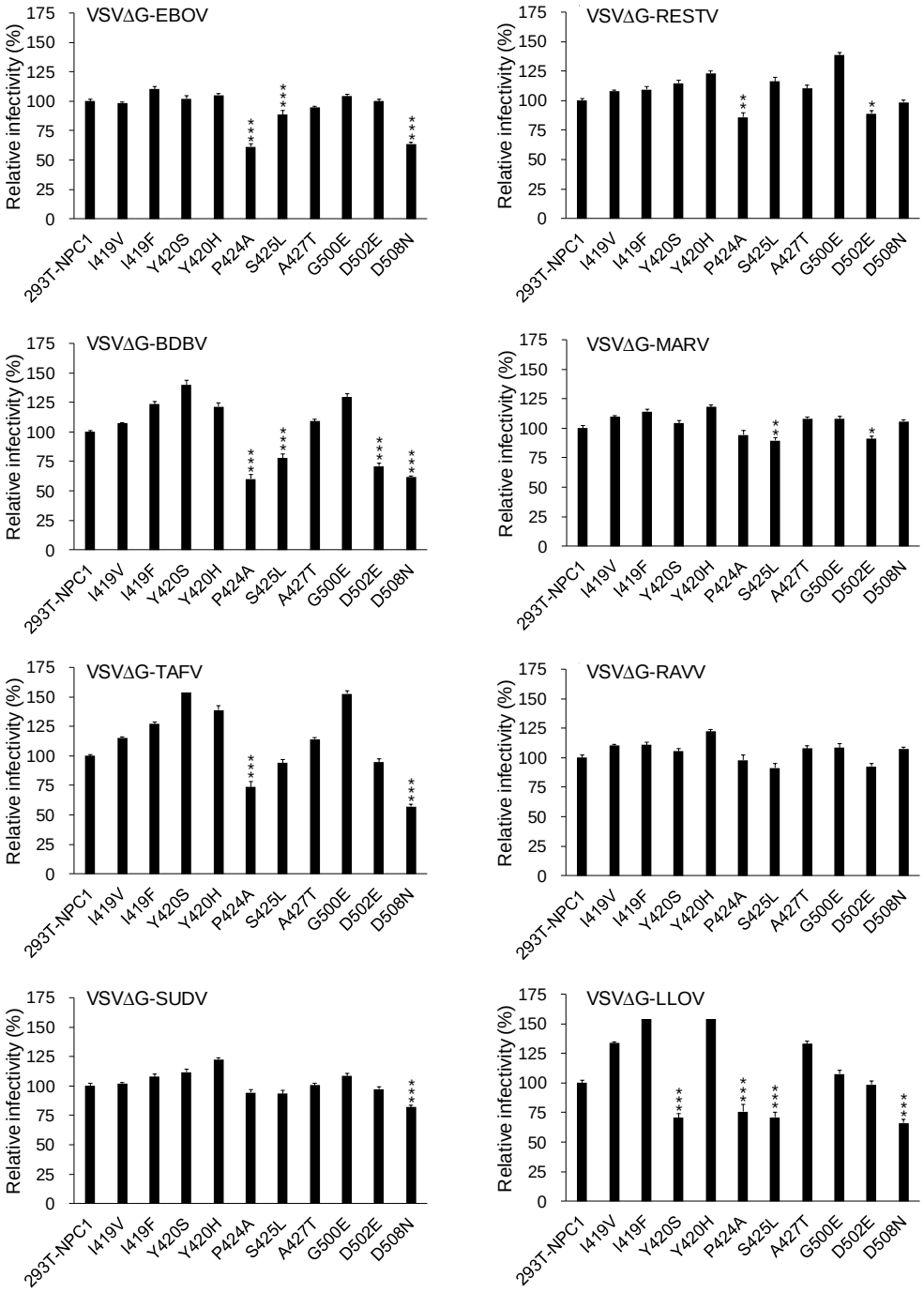

Fig. 7. Infectivities of VSVs pseudotyped with filovirus GPs in Vero E6 cell lines. Each cell line was infected with VSVΔG-EBOV, VSVΔG-BDBV, VSVΔG-TAFV, VSVΔG-SUDV, VSVΔG-RESTV, VSVΔG-MARV, VSVΔG-RAVV, and VSVΔG-LLOV. Relative infectivity in each cell line was calculated by setting the IU value of cl.19 cells expressing 293T-NPC1 to 100%. The means and standard errors of thirty replicates are shown. Values significantly lower than those for 293T-NPC1 cells are shown (*$P < 0.05$, **$P < 0.01$, ***$P < 0.001$).

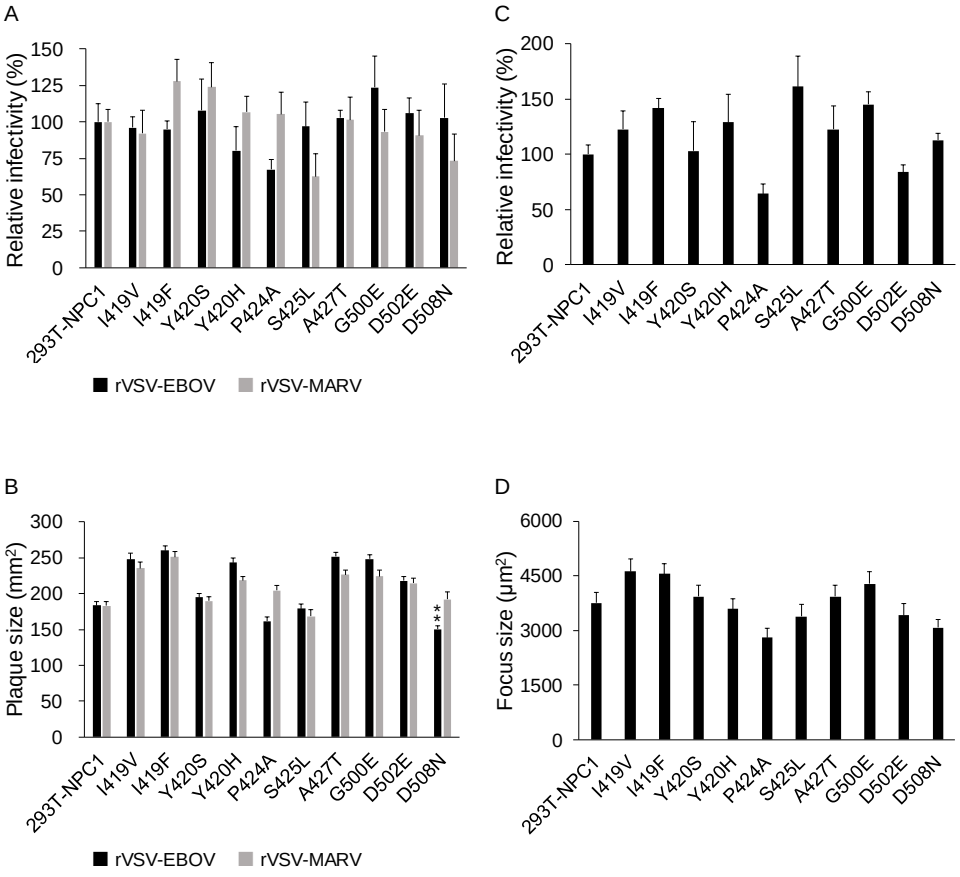

Fig. 8. Plaque/focus formation of rVSV-EBOV, rVSV-MARV, and EBOV-GFP in Vero E6 cell lines. (A) rVSV-EBOV and rVSV-MARV were inoculated into Vero E6 cells and incubated at 37°C for 3 days with 1.0% agarose in maintenance medium. The cells were stained with 0.5 % crystal violet in 10% formalin and the PFUs in each cell line were quantified by counting the number of visible plaques. The data represent the means and standard errors of at least three independent experiments. (B) Plaque sizes were measured using the Image-J software. The means and standard errors of 50-100 plaques per well are shown. (C) Confluent monolayers of Vero E6 cells were inoculated with EBOV-GFP and incubated at 37°C for 3 days with 1.2% carboxymethyl cellulose in maintenance medium. The cells were fixed and the GFP foci in each cell line were counted under a fluorescence microscope. The data represent the means and standard errors of triplicate assays. (D) The sizes of the foci were measured using the Image-J software. The means and standard errors of 60-150 foci per well are shown. (A-D) Values significantly lower than those for 293T-NPC1 cells are indicated (*$P < 0.05$, **$P < 0.01$, ***$P < 0.001$).

Reduced focus-forming ability of EBOV in Vero E6 cells with the P424A substitution

To examine the effects of substitutions associated with NPC1 SNPs on actual filovirus infection, I used an infectious EBOV expressing GFP and determined the viral focus numbers and average focus size in each cell line. Consistent with my pseudotyped VSV data, the P424A substitution resulted in reduced focus numbers of EBOV-GFP (Fig. 8C). The average size of foci in this cell line was also smaller than that in cells expressing 293T-NPC1 (Fig. 8D). Although these differences were not significant in a multiple comparison analysis, Welch's *t*-test yielded significant differences, compared to the case for 293T-NPC1-expressing cells. The D508N substitution slightly reduced the focus size of EBOV-GFP, but there was no statistically significant difference compared to the focus size in 293T-NPC1-expressing cells.

DISCUSSION

With regards to human immunodeficiency virus type 1 (HIV-1) infection, there are a subset of people who are inherently resistant to the virus[54,72,74,82]. In particular, genetic variation in the host viral receptors has been shown to reduce the susceptibility to HIV infection in humans[54,82]. Although there are only a few studies regarding asymptomatic filovirus infection, Baron *et al*.[4] reported potential asymptomatic cases during the outbreak in Sudan in 1979, and Dean *et al*.[18] estimated the proportion of asymptomatic transmissions during the recent epidemic in West Africa. Relationships among host genetics, Ebola virus disease progression, and resistance have been studied in mice[34,78]; however, the details of genetic polymorphisms that may affect the susceptibility of humans to filoviruses have not yet been elucidated.

In the present study, I focused on 10 reported NPC1 SNPs that interact with GP. Although none of the SNPs tested here completely ablated viral entry or infectivity, some SNPs were, nevertheless, found to be important for filovirus infection. In my experiments, the P424A substitution reduced the entry of VSV pseudotyped with ebolavirus, but not marburgvirus GPs. Moreover, the sizes of the foci of EBOV-GFP were also reduced in this cell line. Interestingly, Wang *et al*.[97] demonstrated that the P424A NPC1 mutant retained its binding capacity to dGP, but with reduced affinity compared to wild-type NPC1. Collectively, these findings suggest that the P424A substitution in NPC1 lowers its binding capacity to dGP, resulting in reduced viral entry and infection.

The S425L substitution also reduced the infection with some pseudotyped VSVs, including VSVΔG-MARV and -RAVV. The serine residue at position 425 in NPC1 was shown to be involved in the interaction with the amino acid residue at position 142 of the EBOV GP molecule[97]. However, since the amino acid residues at this position are

different in EBOV and MARV GPs (serine at position 142 of EBOV GP and glutamine at position 126 of MARV GP), the effects of the S425L substitution may be different between EBOV and MARV. It has also been demonstrated that single amino acid mutations at positions 502 or 503 in NPC1 can reduce viral infection[68,70]. My experiments confirmed this finding, as the D502E substitution reduced the entry of some of the pseudotyped viruses I tested and also reduced infection with EBOV-GFP (but not significantly). Notably, while the previous study introduced a significant loss of charge at residue 502 by mutating the aspartic acid to phenylalanine[70], my study shows that even a minimal variation at this residue (D to E) can have an effect on viral entry.

Some other amino acids that are also important for binding to dGP have not been reported as SNP sites in the two loops[97]. The rapid increase in the amount of sequence data in public databases may provide additional information on the NPC1 SNP substitutions not evaluated in this study. In fact, the latest dbSNP lists novel SNPs that are not tested here (Table 4). It is also of interest to investigate multiple SNP substitutions in the loops. Although more specific studies are needed to further assess the capacity of NPC1 variation to influence filovirus infection, identifying genetic variations that affect the susceptibility of hosts to filoviruses will be crucial in understanding filovirus disease progression and host cell restriction.

Table 4. SNPs listed in the latest public database (dbSNP)

rsID	Codons	Position in the protein	Amino Acid	Symbol
rs1452719623	ATT/ATG	419	I/M	I419M
rs904005729	TAC/TGC	423	Y/C	Y423C
rs1215387384	GGG/AGG	500	G/R	G500R
rs483352885	GAC/GTC	501	D/V	D501V
rs1416446081	GAC/AAC	502	D/N	D502N
rs143797098	CCT/TCT	424	P/S	P424S
rs1312272396	GTG/GGG	505	V/G	V505G
rs866200919	GCC/GTC	507	A/V	A507V
rs1190383931	TAC/TCC	509	Y/S	Y509S
rs1170655145	CAC/CAG	510	H/Q	H510Q

Summary

NPC1 is responsible for filovirus entry into the host cells because the interaction between filovirus GP and NPC1 is believed to be essential for triggering membrane fusion. While previous studies have determined the residues on NPC1 that are important for binding to GP, mutations in these residues did not reflect a genetic variation of human NPC1. I focused on SNPs in human NPC1, and found that the two loops on domain C of NPC1 that interface with GP had 10 naturally occurring missense SNPs. Here, I demonstrated that some SNPs in human NPC1 may affect filovirus entry into the host cells. Especially, the P424A/D508N and S425L/D502E substitutions seemed to be important for the reduced entry of ebolavirus and marburgvirus, respectively. Although I could not detect any SNPs that completely abolish the viral entry, the recent increase in the amount of sequence data in public databases may contribute towards the detection of these SNPs. In addition to database updating, more sensitive analyses will be required to further assess the capacity of NPC1 variation to influence filovirus infection. As well as interactions between CCR5 variants and HIV-1, NPC1 variations related to asymptomatic filovirus infection would be very interesting findings.

Chapter II:

Putative endogenous filovirus VP35-like protein potentially functions as an IFN antagonist, but not a polymerase cofactor

Introduction

It has been proposed that some nucleotide sequences that are closely related to genes from non-retroviral RNA viruses are found in vertebrate genomes[6,36]. Although the biological significance of these genomic sequences is largely unknown, it was particularly noted that the expression of an endogenous bornavirus-like nucleoprotein element (EBLN) found in the ground squirrel genome, which is one such host genomic sequence, renders oligodendroglial cells resistant to the viral infection[24]. Several studies have further reported that the transcription of human EBLN-1 is responsible for regulating the gene expression of host cells[33,65,84]. These observations suggest that the expression of EBLNs has some beneficial roles, like those of endogenous retroviruses (ERVs) in animal genomes (e.g., syncytin-1 and -2, syncytin-A, -B)[7,19,60]. However, hyperexpression of an ERV, multiple sclerosis-associated retrovirus (MSRV), whose envelope gene shares >93% similarity with syncytin-1, is thought to be involved in multiple sclerosis[57,58]. It has also been reported that the expression of syncytin-1 or the MSRV envelope protein in astrocytes or peripheral blood mononuclear cells is associated with a proinflammatory and autoimmune cascade[1,80]. These observations suggest that ERVs have a variety of effects on cell physiology.

Endogenous filovirus-like elements (EFLs) have also been discovered in several mammalian (e.g., tarsier, opossum, wallaby, and bat) genomes[6,92,93,94]; however, the potential roles of EFLs in filovirus replication have not been elucidated. It is speculated

that some EFLs (e.g., mlEFLN, meEFLN, tsEFL35, and mlEFL35) have been present in the host genome for over 20 million years[6], and the presence of EFLs in host genomes suggests that they may be correlated with cellular susceptibility to filovirus infection[6,94]. Of these EFLs, an endogenous filovirus VP35-like element found in the little brown bat (*Myotis lucifugus*), mlEFL35, has a nearly full-length open reading frame (ORF) corresponding to the VP35 gene[6].

EBOV VP35 has been shown to bind double-stranded RNA (dsRNA) and inhibit type I IFN production (Fig. 2A)[9]. IFNs are a group of signaling proteins released from host cells in response to the presence of several pathogens. Viral infections commonly induce the production of type I IFNs, which interfere with viral replication in infected cells, resulting in the restriction of viral propagation. EBOV replication was also shown to be inhibited by the IFN response induced by RIG-I activation in cell culture[85]. It has been shown that EBOV VP35s impair human IFN-β promoter activation by inhibiting the function of RIG-I, IFN-β promoter stimulator 1 (IPS-1), and TANK-binding kinase 1 (TBK1)[5]. Furthermore, the replication of EBOV possessing a VP35 with a reduced ability to bind dsRNA is significantly attenuated in mice[31]. Thus, VP35s have been thought to be important factors in the pathogenesis of ebolavirus infection. In addition to its function as an IFN inhibitor, VP35 is known as an essential cofactor in the viral polymerase complex of filoviruses (Fig. 2B)[64]. Four viral proteins, NP, VP35, VP30, and L, are major structural components of the nucleocapsid complex and are involved in viral replication and transcription[23,64]. VP35 interacts with NP and L in this complex, and both VP35-NP and VP35-L interactions are believed to be essential for viral RNA synthesis[43,48,64,76,96].

Since there is no information on the natural expression of mlEFL35/mlEFL35p in the little brown bat[93,94], the potential roles of mlEFL35 are completely unknown. To

investigate the potential functions of mlEFL35, I constructed plasmids expressing the putative mlEFL35-derived protein (mlEFL35p) in cultured cells and performed functional analyses to evaluate the potential of mlEFL35p as an IFN antagonist and/or polymerase cofactor. Here, I show that mlEFL35p, as is the case with EBOV VP35, inhibits the RIG-I-mediated signaling pathway and the production of IFN-β, but does not act as a polymerase cofactor or dominant-negative inhibitor.

Materials and Methods

Bioinformatics

The nucleotide sequences of mlEFL35 shown in NCBI (Accession numbers: JN847697 and JN847701) were partial ORFs. To acquire its full-length ORF, I obtained the genomic sequence between the 5'-target site duplication (TSD) and 3'-TSD from the Ensemble database (http://www.ensembl.org/index.html), since the full-length mlEFL35 ORF was reported to be located between these TSDs[6,36]. The obtained sequence (1944 nucleotides) was analyzed using the NCBI BLASTX program in the non-redundant protein sequence database; it was found to contain the mlEFL35 full-length ORF encoding the mlEFL35p that showed high sequence similarities to ebolavirus VP35s with low expectation values. Next, I used the NCBI BLASTP program in the PDB to confirm that the amino acid sequence of mlEFL35p matched with the structure of EBOV VP35. The amino acid sequences were aligned using MAFFT[40] (https://mafft.cbrc.jp/alignment/software/).

Cell culture and construction of plasmids

HEK293 cells (ATCC® CRL-1573™), HEK293T cells (ATCC® CRL-3216™), Vero E6 cells, and Plat-GP cells were grown in DMEM containing 10% FCS. The cells were incubated in a humidified 5% CO_2 incubator at 37°C. The complementary DNA (cDNA) encoding the mlEFL35 ORF was synthesized and cloned into a pUCFa vector (FASMAC). The cDNA encoding mlEFL35p fused to an HA or FLAG tag at the N terminus was cloned into the mammalian expression vector pCAGGS using an In-Fusion cloning kit (BD Clontech). Similarly, the expression plasmids for N-terminally HA- or FLAG-tagged VP35 and NP of an EBOV (Mayinga) or a RESTV (Pennsylvania) were

constructed. The ORF of the NS1 protein of influenza A virus (strain PR8) with a splice acceptor site mutation[91] was C-terminally fused with an HA tag and cloned into pCAGGS. The EBOV minigenome plasmid containing the firefly luciferase gene, p3E5E-luc[98], was also synthesized and cloned into a pUCFa vector (FASMAC). Similarly, the NP, VP35, VP30, VP24, and L genes of EBOV (Mayinga) were cloned into pCAGGS. The cDNA encoding the mlEFL35p/EBOV VP35 chimeric protein was established and cloned into pCAGGS using an In-Fusion cloning kit (BD Clontech). The expression vectors used to produce human IPS-1 have been described previously[41]. The human TBK1 gene was also cloned into pCAGGS. The cDNA encoding HA-tagged mlEFL35p, EBOV VP35, and RESTV VP35 were also cloned into a pMXs-puro vector.

Western blotting for the detection of the expressed proteins

Each cell lysate was mixed with 2× SDS-PAGE sample buffer (Bio Rad) and incubated at 65°C for 15 min. The expressed proteins were separated on a SDS-polyacrylamide gel (Wako) and transferred onto PVDF membranes (Merck). PBS containing 3% (wt/vol) skim milk (Becton Dickinson) and PBST were used as the blocking and wash buffers, respectively. The PVDF membranes were incubated with an anti-HA monoclonal antibody (abcam, ab1424), anti-β actin monoclonal antibody (abcam), or VP24-specific mouse antiserum, which were produced with the synthetic peptide corresponding to the amino acid positions 3-15 (KATGRYNLISPKK) of EBOV VP24, for 60 min, washed with PBST, and then incubated with HRP-conjugated goat anti-mouse IgG (Jackson ImmunoResearch) for 60 min. After washing with PBST, the bound antibodies were visualized with Immobilon Western (Millipore) system.

Indirect immunofluorescence assay

HEK293T cells were seeded onto eight-well chamber slides (Watson) precoated with poly-L-lysine (Cultrex). One day after seeding, the cells were transfected with the plasmids encoding mlEFL35p using the TransIT LT1 reagent (Mirus), according to the manufacturer's instructions. At 24 hours post-transfection, the cells were fixed in 4% (wt/vol) paraformaldehyde for 15 min, and permeabilized by incubation with PBS containing 0.4% (vol/vol) Triton X-100 for 5 min. The following procedures were performed at room temperature. The cells were incubated with PBS containing 1% (wt/vol) BSA, followed by incubation with the anti-HA antibody (abcam) for 60 min. After washing with PBST, the cells were incubated with Alexa Fluor 488-conjugated goat anti-mouse IgG (Molecular Probes, A11001) for 30 min in the dark. The nuclei were stained using 1 μg/ml DAPI (Molecular Probes) for 10 min in the dark. Images were acquired with a 63 × oil objective lens on a Zeiss LSM700 inverted microscope and using the ZEN 2009 software (Carl Zeiss).

Immunoprecipitation (IP) assay

HEK293T cells were transfected with the plasmids encoding HA- and/or FLAG-tagged VP35 and mlEFL35p using the TransIT LT1 reagent (Mirus) according to the manufacturer's instructions. For the expression of NP, pCAGGS plasmids encoding untagged NPs were used. Two days after the transfection, the cells were lysed with cold lysate buffer (50 mM Tris-HCl [pH 8.0], 150 mM NaCl, 2 mM EDTA, 10% glycerol, and 0.05% NP-40) containing an EDTA-free protease inhibitor (Roche). To facilitate the disruption of the cells, the cell suspensions were frozen at -20°C. The samples were then centrifuged at 10000 ×*g* and 4°C for 10 min. The supernatants were mixed with EZview Red Anti-HA Affinity Gel beads (Sigma) and incubated at 4°C overnight with gentle

rocking. After washing the beads with the lysis buffer, they were mixed with HA-peptides (Sigma, 100 μg/ml), followed by incubation at 4°C for 15 min with gentle rocking to elute the HA-tagged protein. The beads were centrifuged at 500 ×*g* and 4°C for 1 min, and the supernatant was mixed with 2× SDS-PAGE sample buffer (Bio Rad) and incubated at 65°C for 15 min. The precipitated proteins were separated on an SDS-polyacrylamide gel (Wako) and transferred onto PVDF membranes (Merck). The HA- or FLAG-tagged mlEFL35p and VP35s were detected using anti-HA tag antibody (abcam) or anti-FLAG tag antibody (Sigma, F1804). The NPs were detected using a mixture of rabbit antiserum specific for EBOV NP (FS0169) and RESTV NP (FS0170)[14]. The bound antibodies were visualized with Immobilon Western (Millipore) system.

Reporter assay for human IFN-β promoter activity

HEK293 cells (1.0×10^5) were seeded onto 12-well plates and transfected with 250, 500, or 1000 ng of each plasmid expressing C-terminally HA-tagged influenza A virus NS1 (IAVs-NS1-HA), N-terminally HA-tagged EBOV VP35 (HA-ZVP35), and RESTV VP35 (HA-RVP35) or mlEFL35p (HA-mlEFL35p), the plasmids for the human IFN-β promoter-driven firefly luciferase reporter gene (pIFNβ-luc, 250 ng, a kind gift from Sonja Best, NIH/NIAID), the Renilla luciferase-based pRL-TK vector (50 ng, Promega), along with the RIG-I caspase activation and recruitment domain (CARD) vector (50 ng/well, a kind gift from Sonja Best), the IPS-1 expression vector (50 ng/well), or the TBK1 expression vector (100 ng/well), using the FuGENE HD transfection reagent (Promega), according to the manufacturer's recommendations. Twenty-four hours after the transfection, the cell culture supernatants were collected and centrifuged at 300 ×*g*, and then stored at -80°C until further use. These cell supernatants were subjected to

enzyme-linked immunosorbent assay (ELISA) to measure the concentrations of human IFN-β. The cells were harvested and lysed in Passive Lysis Buffer (Promega), and then, luciferase assays were performed using the Dual-Luciferase Reporter Assay System (Promega), according to the manufacturer's directions. These cell lysates were subjected to electrophoresis on an SDS-polyacrylamide gel (Wako), followed by Western blotting, to examine the expression of each protein. The firefly luciferase values were normalized to the renilla luciferase values. The normalized values were then compared to the values of the negative control (no induction), to obtain the fold induction values. The results are presented as the percent induction in comparison to the positive control (with only the HA-tag expression vector), the value for which was set to 100%.

Human IFN-β ELISA

The quantitation of IFN-β was performed using a VeriKine-HS Human Interferon Beta Serum ELISA Kit (PBL Assay Science). All procedures were performed according to protocol A of the manufacturer's instructions. The optical density at 450 nm (OD450) was measured using the SoftMax® Pro 6.2.1 software (Molecular Devices). The standard curve was obtained by plotting the OD450, and then, the concentrations of IFN-β (pg/ml) in the samples were calculated.

Minigenome reporter assay

HEK293T cells (5.0×10^4) were seeded onto 24-well plates and then transfected with 50, 100, or 200 ng of plasmids encoding the HA tag alone, HA-ZVP35, or HA-mlEFL35p, along with expression plasmids for the production of EBOV NP (50 ng), VP30 (30 ng), L (400 ng), p3E5E-luc (100 ng), and the T7 polymerase (100 ng), using the TransIT LT1 reagent (Mirus). Further studies with mlEFL35p/EBOV VP35 chimeric

proteins were also performed as described above. In another experiment, HEK293T cells (5.0×10^4) were seeded onto 24-well plates and transfected with 50, 100, or 200 ng of plasmids encoding the HA tag alone, HA-mlEFL35p, or EBOV VP24, along with expression plasmids for the production of EBOV NP (50 ng), VP35 (50 ng), VP30 (30 ng), L (400 ng), p3E5E-luc (100 ng), and the T7 polymerase (100 ng), using the TransIT LT1 reagent (Mirus). At 36 hours after transfection, the cells were lysed using Passive Lysis Buffer (Promega), and the luciferase activity was measured using the Bright-Glo luciferase assay system (Promega), according to the manufacturer's instructions. These cell lysates were also subjected to electrophoresis on an SDS-polyacrylamide gel (Wako), followed by Western blot analysis to examine the expression of each protein. The firefly luciferase activity values were compared to the negative control (without EBOV L expression vector) values to obtain the fold luciferase activity values and the relative luciferase activities were determined by setting the values of the control cells to 100%.

Viruses and Biosafety

Authentic EBOV (Mayinga) was propagated in Vero E6 cells and stored at -80°C. All infectious work with EBOV was performed in the BSL-4 at the Integrated Research Facility of the RML, Division of Intramural Research, NIAID, NIH, Hamilton, Montana, USA. All SOPs were approved by the IBC in the NIH.

Generation of mlEFL35p-expressing cell line

To generate the retroviruses, Plat-GP cells were co-transfected with pMXs-puro encoding HA-mlEFL35p, HA-ZVP35, or HA-RVP35, and the expression plasmid pCAGGS encoding VSV-G cDNA, using the FuGENE HD transfection reagent (Promega), according to the manufacturer's recommendations. Two days later, the culture

supernatants containing retroviruses were collected, and filtered through 0.45-μm filters. HEK293 cells were transduced with retroviruses expressing the mlEFL35 and VP35 genes. Cell lines stably expressing each protein were selected by culturing the cells in DMEM containing 10% FCS and 20 μg/ml puromycin (Sigma).

Growth kinetics of EBOV in cell lines stably expressing mlEFL35p

Each stable cell line was infected with EBOV at an MOI of 0.1. After adsorption for 1 hour, each inoculum was aspirated, and the cells were washed and cultured in DMEM containing FCS (10%), penicillin (100 U/ml), and streptomycin (0.1 mg/ml)at 37°C; culture supernatants were collected at 24-hour intervals. The titers of viruses released into the cell culture supernatants were determined by tissue culture infectious dose for 50% ($TCID_{50}$) assays in Vero E6 cells.

Western blotting for the detection of virus particles

Each supernatant was mixed with 2× SDS-PAGE sample buffer (Bio Rad) and incubated at 95°C for 5 min. The viral proteins were separated by electrophoresis on an SDS-polyacrylamide gel (Wako) and transferred onto PVDF membranes (Merck). PBS containing 3% (wt/vol) BSA and PBST were used as the blocking and wash buffers, respectively. The PVDF membranes were incubated with EBOV NP-specific rabbit antiserum (FS0169), or mouse monoclonal antibodies against the EBOV VP40 protein (ZVP40 29-3) for 60 min, washed with PBST, and then incubated with HRP-conjugated goat anti-mouse IgG (Jackson ImmunoResearch) and HRP-conjugated goat anti-rabbit IgG (KPL) for 60 min. After washing with PBST, the bound antibodies were visualized with Immobilon Western (Millipore) system.

Statistical analysis

All analyses were performed using the R software. One-way ANOVA was performed, followed by a post-hoc paired Student's *t*-test with Bonferroni adjustment for multiple comparisons. *P*-values less than 0.05 were considered statistically significant.

Results

mlEFL35p and ebolavirus VP35s partially share the primary structure

I first confirmed that mlEFL35p showed sequence similarities to ebolavirus VP35s with low expectation values; the highest score was shown by RESTV VP35 (Table 3 and Text). I then compared the amino acid residues involved in three subdomains mapped on filovirus VP35 sequences: the N-terminal domain containing the NP-binding peptide (NPBP) at amino acid positions 20-48 (EBOV numbering)[43,48], the middle oligomerization domain at amino acid positions 82-118 which is required for VP35 homo-oligomerization[63,79], and the C-terminal domain, which is called the IFN inhibitory domain (IID)[50,51,76], at amino acid positions 220-340 (Fig. 9). I found that in mlEFL35p, the NPBP[43,48,53] and the 8-kDa cytoplasmic dynein light chain (LC8)-binding motif[55] in the N-terminal domain were not conserved. Basic amino acid residues at positions 222, 225, 248, and 251 (EBOV numbering) consisting of the first basic patch (FBP) region, which is important for the polymerase cofactor activity[76], were not conserved. Furthermore, of the nine amino acids (i.e., positions 225, 235, 239, 248, 251, 282, 283, 298, and 300), which have been shown to play a critical role in the polymerase cofactor activity[50,76], only two, i.e., those at positions 239 and 283 (EBOV numbering) were conserved. Interestingly, despite the fact that a BLASTP hit was seen for EBOV VP35 (Table 3), four of the five cysteine residues at positions 135, 247, 275, and 326 (EBOV numbering), were not conserved. Cysteine residues are frequently conserved among evolutionary related proteins that have similar structures[98]. However, leucine residues at positions 93 and 107 (EBOV numbering), both of which are important for VP35 homo-oligomerization[79], were conserved among these proteins. Four (i.e., positions 312, 319, 322, and 339) of the six amino acid residues forming the dsRNA-binding site of the IID

Table 3 BLAST search data of mlEFL35.

Program	Query	Database	Subject (Accession Number)	Score	Query cover	E-value†	Identity
NCBI BLASTX	mlEFL35	Non-redundant protein sequences	RESTV VP35 (ACT22800)	125	93%	$3e^{-30}$	32%
NCBI BLASTX	mlEFL35	Non-redundant protein sequences	TAFV VP35 (YP_003815424)	104	92%	$3e^{-22}$	30%
NCBI BLASTX	mlEFL35	Non-redundant protein sequences	SUDV VP35 (ACR33188)	102	93%	$7e^{-22}$	31%
NCBI BLASTX	mlEFL35	Non-redundant protein sequences	BDBV VP35 (AGL73451)	102	91%	$1e^{-21}$	33%
NCBI BLASTX	mlEFL35	Non-redundant protein sequences	EBOV VP35 (AKC36417)	102	79%	$1e^{-21}$	33%
NCBI BLASTP	mlEFL35p	PDB	EBOV VP35 (3FKE_A)	84.3	40%	$4e^{-20}$	38%

†E-value: Expectation-value

Text

mlEFL35 (846 nt)

```
                    20                  40                  60                  80
  1 - ATGTCCCTGGAGCAGTGCAT CGAACAGATAAGTAAGCTCA CCGATCGCTGTGATAGAATC AAAGAAGGCATGACATCTCT TGTAAGCTGCATGGAAAAGC - 100
101 - AGTTTGTTATAATGGATCAT CTCGTAGCTGCCCAGATGGA GATAAAAGCAGATCAAGTCG ATTTTAGTCAGAGTCTTCTG TCTACGTCTTCTAAGGTTAA - 200
201 - TCAACTAGTAGAGAATTTGT CTGAGCTTTTAGCCAAGCTT AGTTATTTGCCTGTAATGTC AGGACCTGCAACATCCACTC TCGAGGCAGCTGGAGCAAAC - 300
301 - ACGCAGGAGCATAGAAGGCC TCCCCCAGGGCCCATCCTAG CAACCCTGGAACGACACGGA GCAAGACCCACAGATACTCT CACTTCTGATATTCCAGGGT - 400
401 - CCGTGAAGGCTGCTGAGGCC GAGAAGAAAATGCATACTGC ACAGACTGTCCCTGGGGAGA GTGTCTCTCGGCTGCCTCTA GTTCCCACCGAATTCGTACG - 500
501 - AGTCCTCACAAGTTATCTGA CAGGACCGCGCACTGCATTT CATGAATTAGTATCGGCAAT CGCTTTGGTGAGCCGAGACT CTCATGATCTACAGGTAGCC - 600
601 - ATGGACCATTTCAATCGAGA GCTAATGGATGGTTTCTCAG CTCATGCTGCCATAATATCC ATCACTCAGAGATGTGAGTA TTTTCGGAACTGCGAAGCTC - 700
701 - CGACAACGCAGGTAACTTCG AAGAGCCAGATTCCACAAGC ATGTCATGGCAGACTTAGGG ATGTACCGGAGGGTCCCAAA ACCCTAGGACGAGGATGGGT - 800
801 - ATATATATATCTAACTCCTG AAGGAAGCCTCGGGTTAAAG ATTTAA                                    - 846
```

mlEFL35p (281 aa)

```
                    20                  40                  60                  80
  1 - MSLEQCIEQISKLTDRCDRI KEGMTSLVSCMEKQFVIMDH LVAAQMEIKADQVDFSQSLL STSSKVNQLVENLSELLAKL SYLPVMSGPATSTLEAAGAN - 100
101 - TQEHRRPPPGPILATLERHG ARPTDTLTSDIPGSVKAAEA EKKMHTAQTVPGESVSRLPL VPTEFVRVLTSYLTGPRTAF HELVSAIALVSRDSHDLQVA - 200
201 - MDHFNRELMDGFSAHAAIIS ITQRCEYFRNCEAPTTQVTS KSQIPQACHGRLRDVPEGPK TLGRGWVYIYLTPEGSLGLK I*                    - 281
```

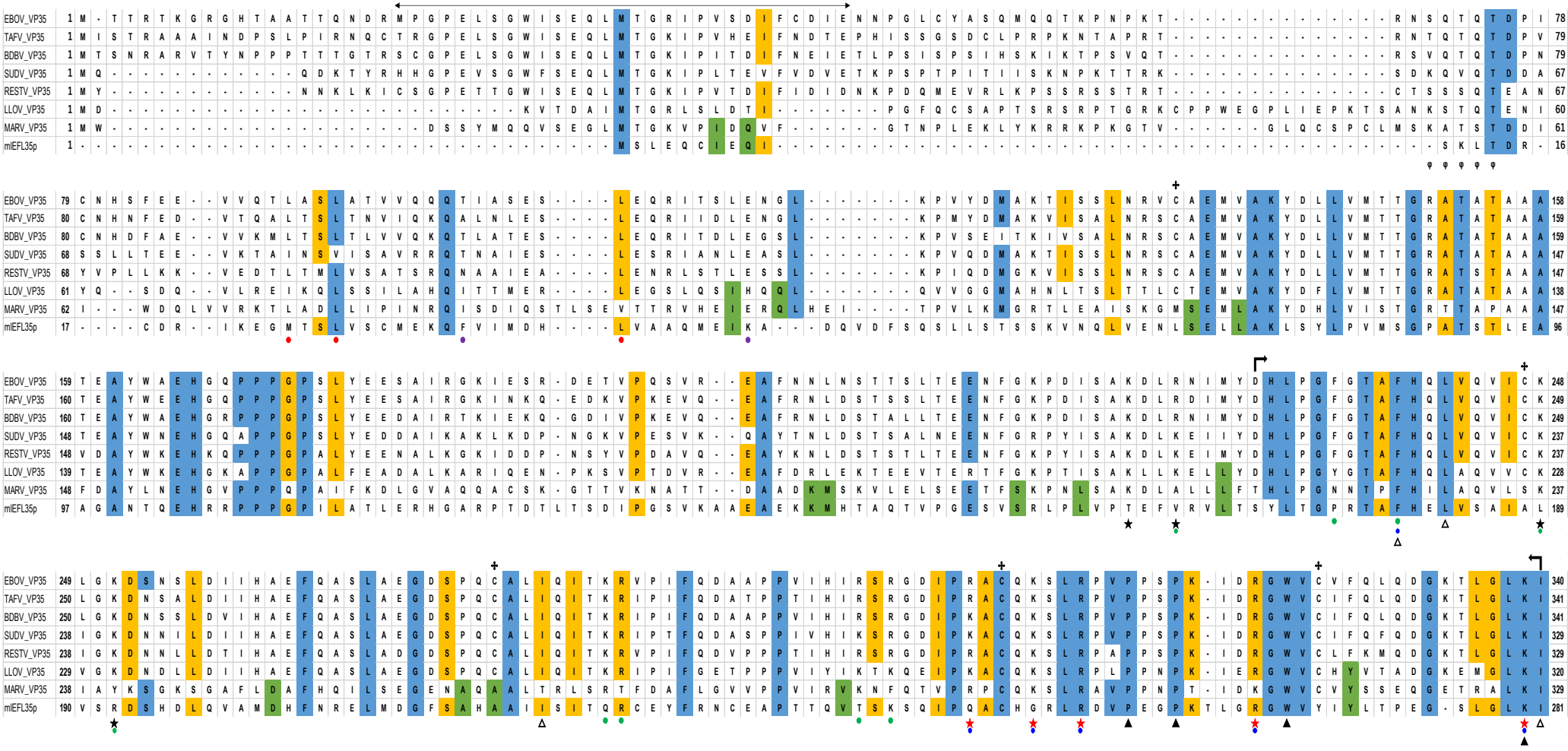
EBOV_VP35
TAFV_VP35
BDBV_VP35
SUDV_VP35
RESTV_VP35
LLOV_VP35
MARV_VP35
mIEFL35p

Fig. 9. Comparison of primary structures of mlEFL35p and filovirus VP35s. The amino acid residues common to VP35s and mlEFL35p are highlighted in blue. The residues featured in yellow represent the amino acids common among ebolavirus VP35s. The residues highlighted in green represent the amino acids common to MARV VP35. The solid line with arrowheads denotes the NPBP of filovirus VP35s[43,48,53]. Phi (φ) represents the s EBOV VP35 LC8-binding motif. The amino acid positions 220-340 (from "↱" to "↰") represent the EBOV VP35 IID[50,51,76]. The amino acid residues indicated by the red and purple dots have been identified to be important for VP35 homo-oligomerization in EBOV and MARV, respectively[63,79]. The amino acid residues indicated by the blue dots and green dots are shown to be critical for the dsRNA-binding and polymerase cofactor activities, respectively[50,76]. The black and red stars indicate the amino acids that form the FBP and the CBP regions on the three-dimensional structure of the VP35 IID, respectively[76]. The black and white arrow heads indicate the amino acids that are important for the folding and stability of VP35 IID[49]. The asterisks (✢) show the cysteine residues in EBOV VP35.

(e.g., the central basic patch [CBP]) were conserved. These findings suggest that mlEFL35p might lack the ability to interact with NP and might limit the ability of VP35 to work as a polymerase cofactor; however, similar to VP35, it might function biologically as an IFN antagonist.

mlEFL35p and VP35s have homo- and hetero-oligomerization potential

I transfected HEK293T cells with the plasmids expressing mlEFL35p and VP35s of EBOV and RESTV and investigated the expression of these proteins by Western blotting and immunofluorescence assays (Fig.10A and 10B). A 30-kDa protein corresponding to the expected molecular weight of mlEFL35p was detected by Western blotting. In the transfected cells, mlEFL35p was detected in the cytoplasm, like the VP35s. Next, HEK293T cells were co-transfected with the expression plasmids for HA- or FLAG-tagged mlEFL35p, VP35s, and/or NP, and the solubilized proteins were immunoprecipitated with each HA-tagged protein. Consistent with previous reports[43,76], I found that FLAG-tagged VP35s were coimmunoprecipitated with HA-tagged VP35s, irrespective of the ebolavirus species, confirming their homo-oligomerization potential (Fig. 11A). Interestingly, FLAG-tagged mlEFL35p was coimmunoprecipitated with not only HA-tagged mlEFL35p, but also the HA-tagged VP35s of EBOV and RESTV (Fig. 11A). I further analyzed the interactions of mlEFL35p with ebolavirus NPs, and found that the EBOV and RESTV NPs were coimmunoprecipitated with the HA-tagged VP35s of the respective viruses, but not with HA-tagged mlEFL35p (Fig. 11B). Collectively, these results reveal that mlEFL35p, like VP35s, had the ability of homo-oligomerization, which might be required for the fundamental functions of VP35. However, consistent with its primary structure, mlEFL35p lacked the ability to interact with NP.

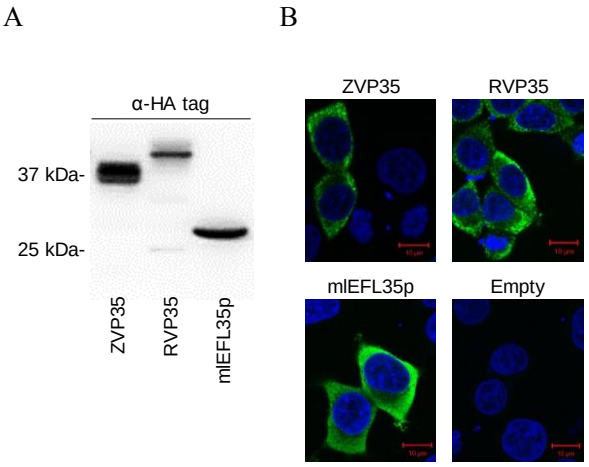

Fig. 10. Expression of the mlEFL35p and VP35s in HEK293T cells. (A) The expression of each protein was confirmed by Western blotting. HA-tagged mlEFL35p (mlEFL35p), HA-tagged EBOV VP35 (ZVP35), and HA-tagged RESTV VP35 (RVP35) were detected as 30-, 37-, and 40-kDa proteins, respectively. (B) The distribution of each protein is visualized by an immunofluorescence assay using anti-HA antibodies. The cells were counterstained with DAPI.

A

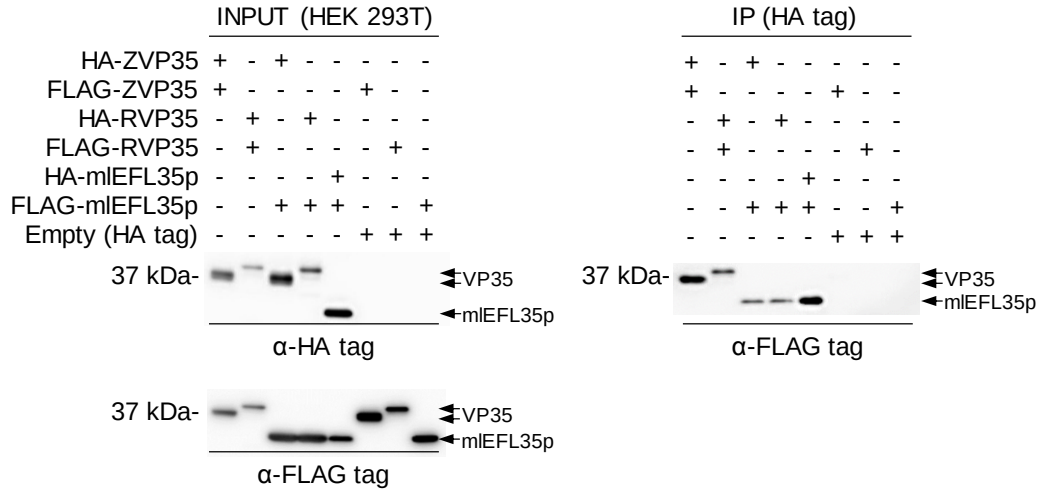

B

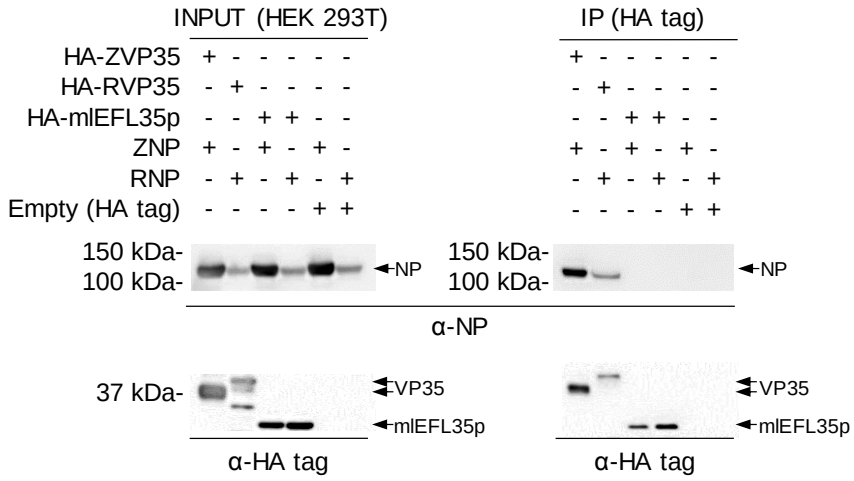

Fig. 11. Immunoprecipitation assay of mlEFL35p, VP35s, and NP. (A) To examine whether mlEFL35p interacted with mlEFL35p itself, EBOV VP35, and RESTV VP35, FLAG-tagged mlEFL35p, EBOV VP35, and RESTV VP35 (FLAG-mlEFL35p, FLAG-ZVP35, and FLAG-RVP35, respectively) expressed in HEK293T cells were immunoprecipitated with HA-tagged mlEFL35p and VP35s of EBOV and RESTV (HA-mlEFL35p, HA-ZVP35, and HA-RVP35, respectively). The precipitated proteins were detected by Western blotting using anti-FLAG tag antibodies. (B) EBOV NP (ZNP) and RESTV NP (RNP) were expressed in HEK293T cells and immunoprecipitated with HA-tagged VP35 of EBOV and RESTV (HA-ZVP35 and HA-RVP35, respectively) or HA-tagged mlEFL35p. Each HA-tagged protein was detected by Western blotting using anti HA-tag antibodies. Similarly, ZNP and RNP were detected using rabbit antisera specific to NPs[14].

mlEFL35p functions as an antagonist that inhibits the RIG-I-mediated signaling pathway

The human IFN-β promoter is known to be activated by RIG-I, IPS-1, and TBK1 (Fig. 12A)[5]. Using a reporter assay with these activators, the anti-IFN activity of mlEFL35p was evaluated by comparing it to influenza A virus NS1 (IAV-NS1), EBOV VP35, and RESTV VP35, all of which are known to act as IFN antagonists (Fig. 12A and 12C)[9,26]. When the human IFN-β promoter activation was induced by RIG-I, mlEFL35p suppressed the IFN-β promoter activity as efficiently as EBOV VP35, but not as well as NS1. IPS-1-triggered IFN-β promoter activation was also inhibited by mlEFL35p to the same extent as that by EBOV VP35. Ebolavirus VP35s and mlEFL35p showed similar effects on TBK1-induced IFN-β promoter activity. I then quantified the IFN-β levels in the supernatants of the transfected cells (Fig. 12B and 12D). Consistent with the results of the reporter assay, the concentrations of IFN-β released into the culture supernatant also decreased in the presence of mlEFL35p. Although a statistically significant difference was observed only between IPS-1-triggered and control cells in the multiple comparison analysis, the expression of mlEFL35p reduced the production of IFN-β significantly or nearly significantly (IPS-1 or TBK1, respectively), when comparisons were made individually between mlEFL35a-expressing cells and negative control cells (Empty). It was noted that the difference in the suppression efficiency between mlEFL35p and VP35s was correlated with that seen in the reporter assay. These results suggest that mlEFL35p could potentially function as an IFN antagonist.

mlEFL35p plays a limited role in EBOV genome transcription and/or replication

I used the EBOV minigenome system[64] to analyze the effects of the mlEFL35p expression on EBOV genome transcription/replication (Fig. 13). I first confirmed that

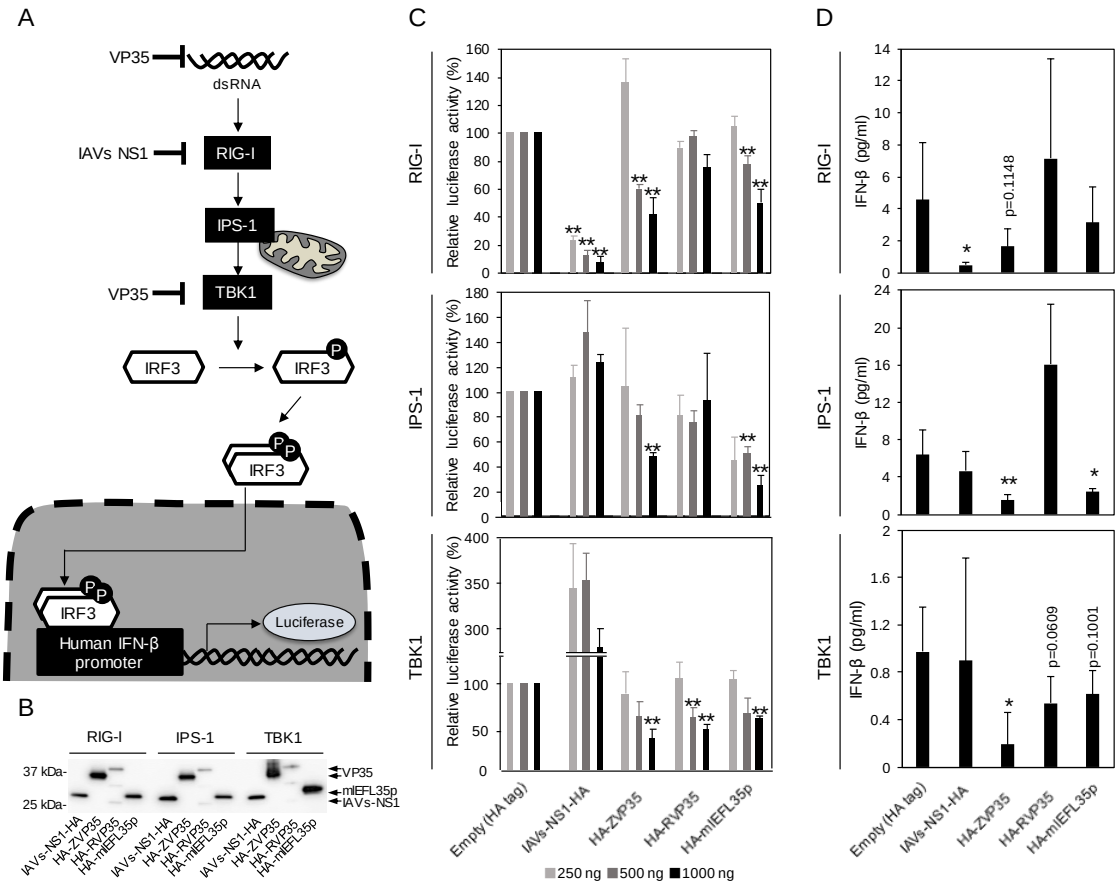

Fig. 12. Inhibition of the RIG-I-mediated signaling pathway by mlEFL35 and VP35s. (A) The RIG-I-mediated signaling pathway is shown. The human IFN-β promoter is activated through RIG-I, IPS-1, and TBK1. The IFN-β promotor activity was measured by luciferase reporter assays. (B) HEK293 cells were transfected with each plasmid expressing HA-tagged influenza A virus NS1 (IAVs-NS1-HA), EBOV VP35 (HA-ZVP35), RESTV VP35 (HA-RVP35), or mlEFL35p (HA-mlEFL35p) and the plasmids for the reporter gene expression along with the RIG-I CARD vector, and the IPS-1 or the TBK1 expression vector. NS1 and VP35 are known IFN antagonists. Western blotting was performed to examine the expression of NS1, VP35s, and mlEFL35p. Each HA-tagged protein (IAVs-NS1-HA, HA-ZVP35, HA-RVP35, and HA-mlEFL35p) was detected using anti-HA-tag antibodies. (C) The transfected cells were solubilized, and luciferase assays were performed. Relative luciferase activities were calculated by setting the values resulting from the cells transfected with a control empty plasmid expressing the HA tag alone to 100%. Significantly lower values compared to control cells (Empty) are indicated by asterisks (*$P < 0.05$, **$P < 0.01$). (D) Concentrations of IFN-β in the supernatants of cells transfected with the represented plasmids (1000 ng) were measured by ELISA. The means and standard deviations of five independent experiments are shown. Significantly lower values compared to control cells (Empty) are indicated by asterisks (*$P < 0.05$, **$P < 0.01$).

EBOV VP35 was required for luciferase expression in this system, and then found that the expression of mlEFL35p, in place of EBOV VP35, induced only background levels of luciferase activity resulting from the empty plasmid (Fig. 13A). I also examined the dominant-negative effects caused by the overexpression of mlEFL35p (Fig. 13B). I found that the expression of EBOV VP24 caused a significant decrease in luciferase activity, as shown previously[98]. In contrast, the expression of mlEFL35p only slightly reduced the luciferase activity. The expression levels of the HA-tagged proteins in the transfected cell lysates were analyzed by Western blotting (Fig. 13C). These results suggest that mlEFL35p might not function as a polymerase cofactor or dominant-negative inhibitor in this human cell line.

To map specific regions of mlEFL35p essential for polymerase cofactor activity, a total of three mlEFL35p/EBOV VP35 chimeric proteins were constructed. In brief, the NPBP derived from EBOV VP35 was fused with mlEFL35p, and the N-terminal and C-terminal domains of EBOV VP35 and mlEFL35p, respectively, were swapped (Fig. 14A). EBOV VP35 functioned as a positive control in the EBOV minigenome assay; however, all chimeric proteins could not work as well as EBOV VP35 (Fig. 14B). These chimeric constructs recapitulated the only background levels of luciferase activity seen for mlEFL35p, preventing me from determining which subdomain was important for polymerase cofactor activity in mlEFL35p.

EBOV replication is not affected by the expression of mlEFL35p in HEK293 cells

The effect of mlEFL35p expression on the *in vitro* replication capacity of EBOV was finally examined. I compared the growth kinetics of EBOV in cell lines stably expressing EBOV VP35, RESTV VP35, or mlEFL35p. The amounts of viral

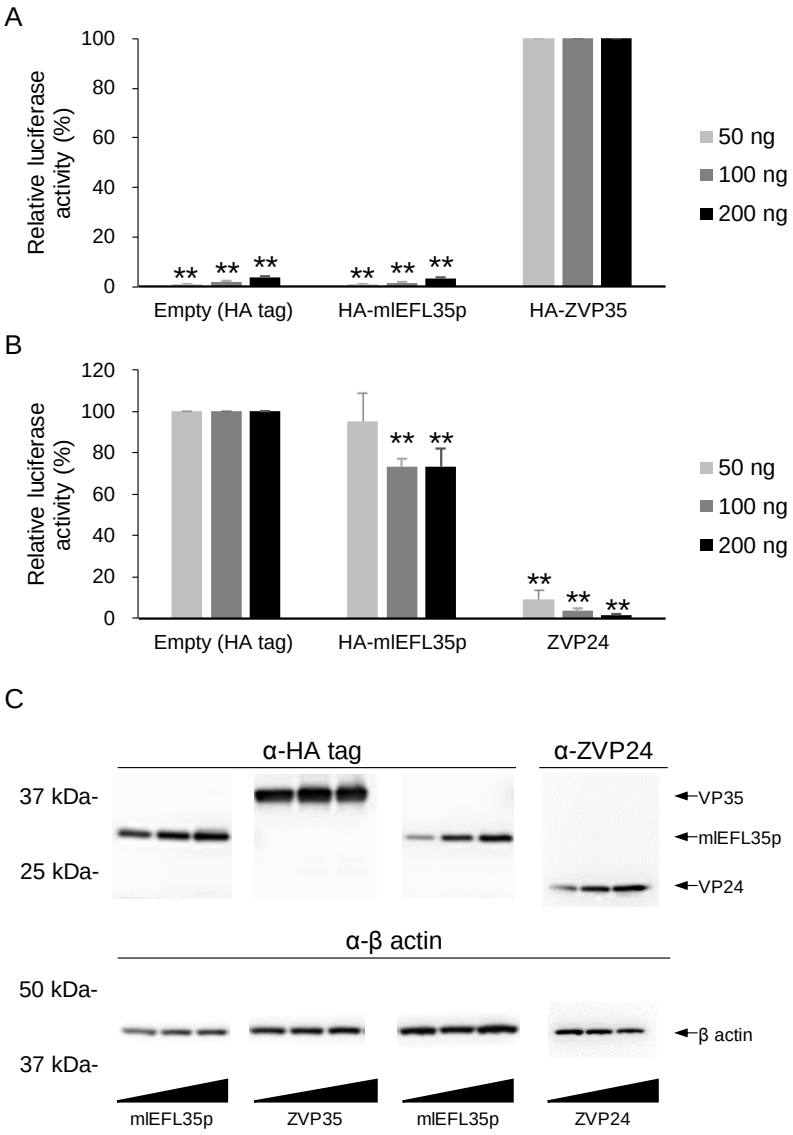

Fig. 13. Luciferase expression from the Ebola virus minigenome with mlEFL35p. (A) HEK293T cells were transfected with the described amounts of plasmids for the expression of the HA tag alone, HA-tagged mlEFL35p (HA-mlEFL35p), or EBOV VP35 (HA-ZVP35), along with plasmids for the expression of EBOV NP, VP30, L, the T7 polymerase, and p3E5E-luc. Relative luciferase activities were determined by setting the values of the control cells transfected with the HA-ZVP35-expressing plasmid to 100%. The means and standard deviations of three independent experiments are shown. Significant differences compared to the values for the control cells (HA ZVP35) are indicated by asterisks (**$P < 0.01$). Between the empty control and mlEFL35p, there was no significant difference. (B) HEK293T cells were transfected with the indicated amounts of plasmids for the expression of the HA tag alone, HA-tagged mlEFL35p (HA-mlEFL35p), or EBOV VP24 (ZVP24), along with plasmids for the expression of EBOV NP, VP35, VP30, L, the T7 polymerase, and p3E5E-luc. ZVP24 was used as a positive control[98]. The means and standard deviations of three independent experiments are shown. Significantly lower values compared to those for control cells (Empty) are indicated by asterisks (**$P < 0.01$). (C) The expression of each protein was detected by Western blotting. The HA-tagged proteins (HA-ZVP35 and HA-mlEFL35p) were detected using anti-HA tag antibodies. ZVP24 was detected using a VP24-specific mouse antiserum. β actin was detected using an anti-β actin antibodies.

A

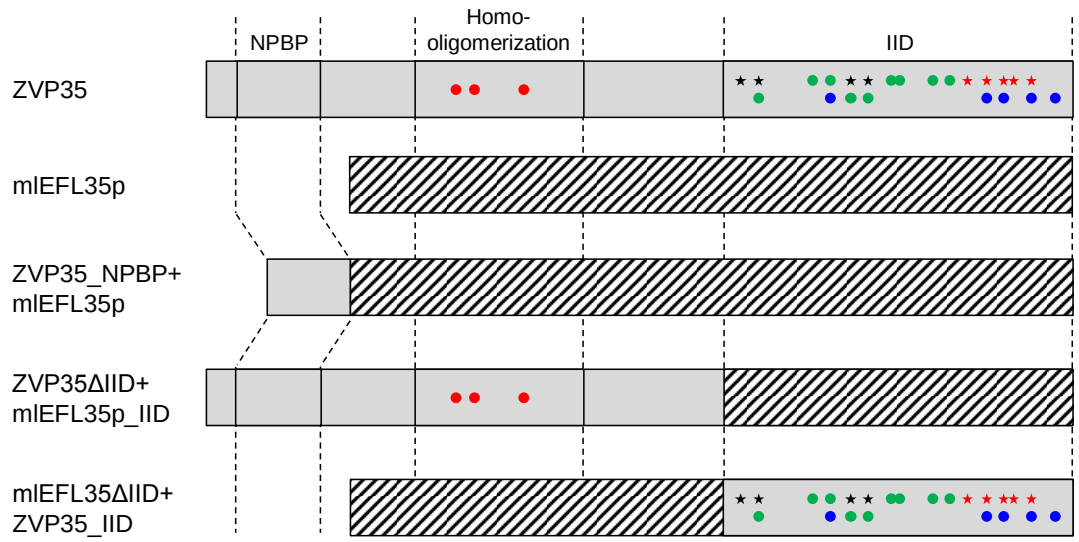

B

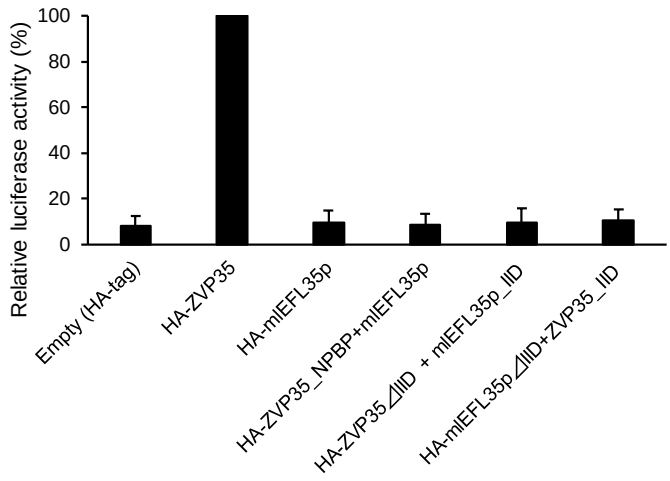

Fig. 14. Luciferase expression from the Ebola virus minigenome with mlEFL35p/EBOV VP35 chimeric proteins. (A) Schematic diagram of EBOV VP35 and mlEFL35p chimeric constructs. The circles and stars represent the key residues shown in Fig. 9. (B) HEK293T cells were transfected with 50 ng of plasmids for the expression of the HA tag alone, HA-tagged mlEFL35p (HA-mlEFL35p), EBOV VP35 (HA-ZVP35), or the chimeric protein described in (A), along with plasmids for the expression of EBOV NP, VP30, L, the T7 polymerase, and p3E5E-luc. Relative luciferase activities were determined by setting the values of control cells transfected with the HA-ZVP35-expressing plasmid to 100%. The means and standard deviations of three independent experiments are shown.

particles released into the supernatant were evaluated by detecting the viral proteins EBOV NP and VP40.The virus titer released into cell culture supernatants was determined by the $TCID_{50}$ assay. These assays enabled me to examine the effect of mlEFL35p on EBOV life cycles; however, I did not find any significant negative effect of mlEFL35p (Fig. 15A and 15B). Stable cell lines expressing mlEFL35p completely supported EBOV replication.

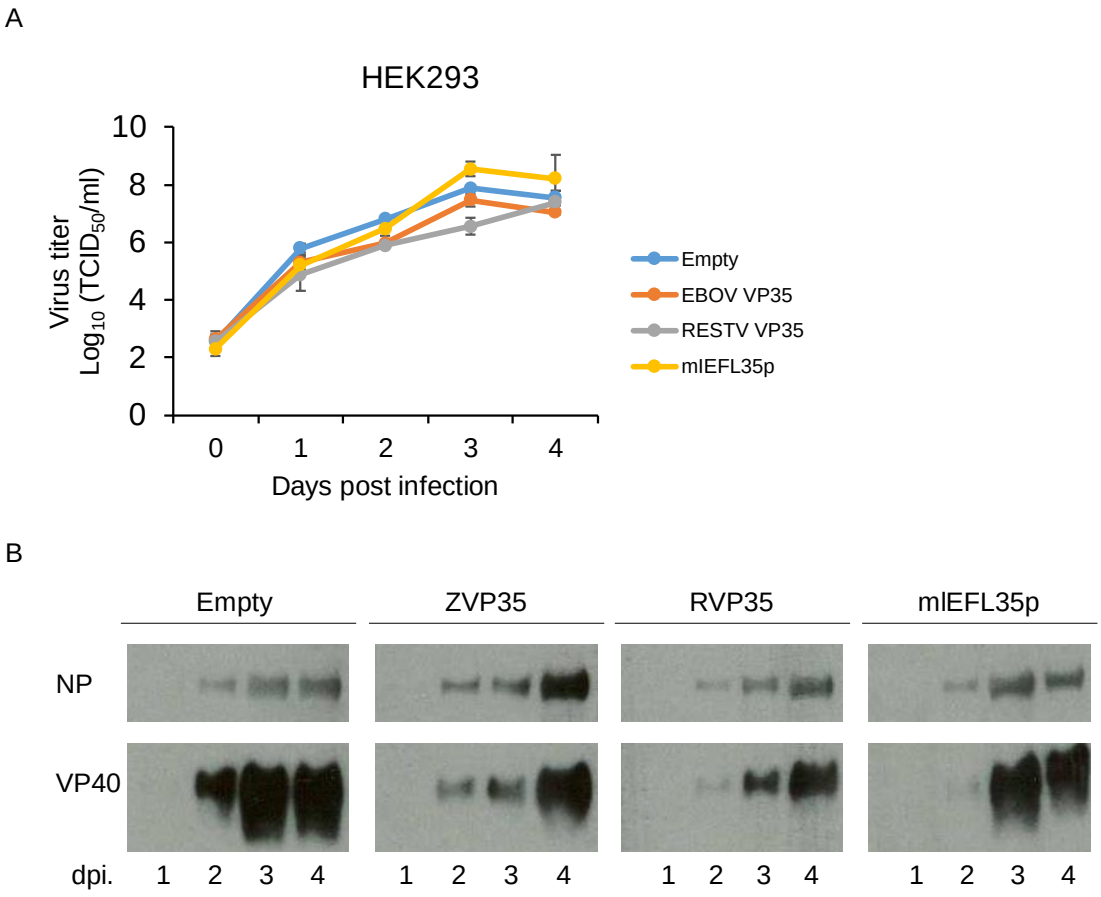

Fig. 15. Comparison of the growth kinetics of EBOV in HEK293 cells. (A) Growth kinetics of EBOV in HEK293 cells stably expressing EBOV VP35, RESTV VP35, or mlEFL35p is compared. All data represent the means and standard errors of triplicate assays. (B) The amounts of viral particles released into the supernatant were analyzed by detecting EBOV NP and VP40. dpi.: days post infection.

Discussion

In this chapter, I determined the full-length mlEFL35-encoding ORF sequence in the genome of the little brown bat (Text), and biologically analyzed the potential functions of the putative protein, mlEFL35p. Comparison of the amino acid sequences between mlEFL35p and VP35s revealed that the primary structure of mlEFL35p showed a high similarity to ebolavirus VP35s. I found that mlEFL35p lacked the NPBP and the LC8-binding motif in the N-terminal domain. Accordingly, I demonstrated that mlEFL35p had the potential to act as an IFN antagonist, but not a polymerase cofactor.

As expected from the primary structure (i.e., conserved leucine residues at positions 93 and 107, four conserved residues in the CBP), mlEFL35p was coimmunoprecipitated with homologous (mlEFL35p) and heterologous (VP35) molecules, suggesting its homo- and hetero-oligomerization potential. It has been shown that the homo-oligomerization of EBOV VP35 is important for its IFN antagonist activity[79]. My data may also suggest a link between the homo-oligomerization of mlEFL35p and its function as an IFN antagonist. In addition, the ability of mlEFL35p to interact with both EBOV and RESTV VP35s strongly suggested that mlEFL35p and VP35s have structural similarities and share some functions. Interestingly, mlEFL35p inhibited the RIG-I-mediated IFN-β production more efficiently than RESTV VP35, and its inhibitory potential was indeed similar to that of EBOV VP35. Although the expression levels of RESTV VP35 seemed to be lower than those of EBOV VP35 and mlEFL35p, since TBK1-triggered IFN-β promoter activation was inhibited as efficiently as EBOV VP35, it is not highly likely that the low expression of RESTV VP35 was a major cause of its lowered inhibitory potential. However, there is no difference between the EBOV

and RESTV VP35s with regards to the amino acid residues that are critical for VP35 homo-oligomerization and the dsRNA-binding site (Fig. 9), both of which are required for the IFN antagonist activity of VP35s[32,79]. Leung *et al*.[51] reported that RESTV VP35 contained an additional helical structure in its IFN inhibitory domain and proposed that the helical structure might increase the stability and decrease the flexibility of the RESTV VP35 molecule. Such a structural difference might influence the IFN antagonist activity. However, Guito *et al*.[29] demonstrated that both the EBOV and RESTV VP35s were similarly potent IFN antagonist proteins. Since differences in experimental conditions (e.g., use of a human codon-optimized ORF of VP35 and different procedures for IFN induction) might cause different effects, further studies are required to clarify whether the anti-IFN potential is involved in the differential pathogenicity of EBOV and RESTV.

It has been demonstrated that VP35 interacts with IRF kinases such as TBK1 and the inhibitor of κB kinase epsilon (IKKε), and the physical interaction between IKKε and either IPS-1, IRF-3, or IRF-7 was impaired by EBOV VP35 overexpression[77]. As shown in Fig. 12, my reporter assay showed that TBK1-induced human IFN-β promoter activity was most significantly inhibited by mlEFL35p, suggesting that mlEFL35p also targets these IRF kinases. EBOV VP35 binds not only dsRNA, but also PKR activator (PACT), both of which are recognized by RIG-I. The ability of VP35 to block PACT activation requires the CBP structure[56]. Comparison of the primary structure of mlEFL35p and ebolavirus VP35s indicates that the majority of amino acids forming the CBP structure are conserved in mlEFL35p. This suggests that like EBOV VP35, mlEFL35p may also inhibit PACT activation.

It was noted that four of the five cysteine residues in VP35s were not conserved in mlEFL35p. Cysteine residues often form a disulphide bond, which plays an important

role in protein folding and stability. Thus, cysteine residues important for protein structures are generally conserved among related proteins[17]. Crystal structure analysis has shown that the cysteine residues at positions 247 and 275 of EBOV VP35 do not form a disulfide bond[49]. Although the structural impacts of the other cysteine residues of VP35 remain unknown, my data suggest that the cysteine residues of mlEFL35p and VP35s are not important for their fundamental function as IFN antagonists.

As suggested by the comparison of the amino acid sequences of mlEFL35p and VP35s (e.g., lack of the NPBP), NP was not coimmunoprecipitated with mlEFL35p. The NP-VP35 interaction has been shown to be essential for viral transcription/replication[64]. Accordingly, my EBOV minigenome reporter assay demonstrated that mlEFL35p could not be substituted for EBOV VP35 in the viral transcription/replication cycle. It was also speculated that the overexpression of mlEFL35p might show dominant-negative effects by forming hetero-oligomers between the mlEFL35p and VP35 molecules. However, mlEFL35p only slightly interfered with the function of VP35, and no detectable effect of mlEFL35p on the EBOV life cycle was observed. These results suggest that mlEFL35p might not have critical functions involved in viral transcription/replication.

It has been proposed that ERVs in animal genomes provide some beneficial effects to host animals and might play important roles in their coevolution[2,3,86]. It has also been demonstrated that non-retroviral elements, EBLNs, are involved in antiviral effects and the regulation of the expression of neighboring genes[24,33,84]. However, in this chapter, I demonstrated that mlEFL35p potentially acts as an IFN antagonist like EBOV VP35, suggesting its suppressive effect on the host immunity. While mlEFL35 was found in an insectivorous bat (*Myotis lucifugus*), there is no information on the susceptibility of this bat species to ebolaviruses. In addition, cell lines of this bat species are also unavailable.

Some species of fruit bats are suspected to be natural hosts[47,73,75,100]; however, it should also be noted that EBOV is able to replicate and cause seroconversion without any symptoms in some insectivorous bat species[87]. Thus, further analyses are required to estimate the impact of mlEFL35p on the host physiology. Overall, previous studies have indicated that many species of bats are susceptible to ebolaviruses. To better understand the potential roles of EFLs in ebolavirus infection, it would be of interest to screen various bat cell lines for the presence of genomic EFLs and to analyze their biological effects by knockdown/knockout experiments using cell lines naturally expressing EFLs. It has been reported that the transcription of human EBLN-1 is responsible for regulating gene transcription[33,65,84]. Thus, it is also important to focus on the function of not only EFL-derived proteins, but also non-coding RNA transcripts. Once cell lines that naturally express EFLs are established, loss-of-function experiments, which are needed for further understanding the biological significance of EFLs in the ebolavirus ecology, could be performed

Summary

Following the discovery of an EBLN, other endogenous non-retroviruses have also been discovered. EFLs have been discovered from the genomes of some species of bats. Since bats have been speculated to play an important role in filovirus transmission without any symptoms, EFLs have been hypothesized to confer resistance to filoviruses in bats. However, extensive studies related to EFLs have not yet been reported. To investigate the potential functions of EFLs, I focused on mlEFL35, which has a nearly full-length ORF corresponding to the filovirus VP35 gene. Here, I show that mlEFL35p, as is the case with EBOV VP35, inhibits the RIG-I-mediated signaling pathway and the production of IFN-β, but does not act as a polymerase cofactor or dominant-negative inhibitor. Though more extensive studies are essential to determine the biological effects of mlEFL35p, mlEFL35p potentially acted as an IFN antagonist, raising the interesting possibility that it may be associated with a suppressive effect on the host immunity.

Conclusion

Filoviruses utilize a variety of cellular proteins for their life cycle (e.g., entry, replication, immune evasion, and egress); however, the detailed mechanisms underlying the filovirus infection have not been fully elucidated yet. Interactions between host factors and viral proteins are closely associated with filovirus pathogenicity and cell tropism. Thus, it is important to understand host molecules involved in the life cycle of filoviruses. In this thesis, I have focused on the mechanisms underlying filoviral cellular entry, replication, and evasion from host immunity.

In chapter I, I have demonstrated that human NPC1 SNPs may influence the susceptibility of cells to filoviruses. Although none of the SNPs tested here completely abolished the filovirus entry into cells, the P424A/D508N and S425L/D502E substitutions seemed to be particularly important for the reduced entry of ebolavirus and marburgvirus, respectively. Due to the rapid increase in the amount of sequence data in public databases, further information on NPC1 sequences will be continuously accumulated in the future, which may enable us to identify additional SNP substitutions affecting filovirus infection. In future studies, it is also important to clarify the impact of combined SNPs and to explore the geographical relationships between NPC1 SNPs and filovirus outbreaks.

In chapter II, I have shown that mlEFL35p, as well as EBOV VP35, potentially antagonizes the RIG-I-mediated signaling pathway and the production of IFN-β, but does not work as a polymerase cofactor or dominant-negative inhibitor. Unlike other endogenous virus-like elements (e.g., EBLN), mlEFL35p partially imitates the biological function of filoviral proteins (e.g., VP35). Unfortunately, there is no information

regarding the natural expressing of mlEFL35p in bats, as well as many other EFLs (e.g., meEFLN, tsEFL35), most of which have not yet been functionally investigated. Thus, more extensive studies are essential to assess the biological importance of EFLs. Future directions of EFL studies should focus on the screening of a large number of cell lines from various animal species for identifying those that naturally express EFLs and on the function of non-coding RNA transcripts expressed from EFLs.

The present thesis provides new insights into the molecular basis underlying filovirus infection and tropisms. I have shown that not only the presence or expression of particular molecules such as virus-specific receptors, but also their SNPs, contributes to cell tropism of filoviruses. This concept will be expanded to many other viruses, since capturing and representing sequencing data from diverse populations, which are in progress around the world, will provide new information regarding the polymorphisms of host cell proteins that affect their interactions with viral proteins. In addition, the present thesis reveals fascinating evidence that like filovirus VP35, mlEFL35p partially retains its ability to inhibit the host immunity. While it is currently difficult to predict the biological roles of mlEFL35/mlEFL35p in bats, this evidence affords the first example that an endogenous non-retrovirus-like element functions like a viral protein.

In the 21st century, the emergence of viral zoonoses has an overwhelming influence on human health and its economic activity. The development of countermeasures is imperative to minimize the impact of zoonoses on human health and economy. To explore potential targets for antiviral treatments, it is crucial to understand the interactions between the viral and host molecules involved in virus life cycles. Further studies in this field will open new avenues for the control of viral zoonoses.

Acknowledgements

I extend my gratitude to my supervisor, Prof. TAKADA Ayato (Division of Global epidemiology, CZC, HU). His comments and suggestions have been extremely valuable during the course of my research. In addition, he has given me a lot of opportunities to participate in overseas activities and attend national conferences. Even when I had numerous queries and faced difficulties with my research, he was kind and approachable to me. I am indebted to him for his consistent patience and understanding towards me throughout this project; under his guidance, I have matured as a researcher.

I sincerely appreciate the support and suggestions provided by Prof. SAWA Hirofumi (Division of Molecular Pathobiology, CZC, HU), Prof. HIGASHI Hideaki (Division of Infection and Immunity, CZC, HU), and Prof. KARIWA Hiroaki (Laboratory of Public Health, Preventive Veterinary Medicine, Division of Veterinary Medicine, Faculty of Veterinary Medicine, HU).

I am deeply grateful to Associate Prof. IGARASHI Manabu (Division of Global epidemiology, CZC, HU). His explanation and proficiency with regards to *in silico* analyses of protein structures and molecular modeling have improved my understanding regarding many aspects of virology. I am also grateful to Assistant Prof. YOSHIDA Reiko, Assistant Prof. MANZOOR Rashid (Division of Global epidemiology, CZC, HU), and Dr. FUJIKURA Daisuke (Division of Infection and Immunity, CZC, HU). They have always taken time out of their busy schedules to help me.

I am also particularly grateful to Dr. MARZI Andrea, Dr. FELDMAN Heinz, Dr. OKUMURA Atsushi, Ms. MENK Key (National Institute of Allergy and Infectious Disease, National Institutes of Health, Rocky Mountain Laboratories), Dr. TSUDA

Yoshimi (Department of Microbiology, Faculty of Medicine, HU), and all the employees at Rocky Mountain Laboratories. It has been my honor to work with them.

I thank the Program for Leading Graduate School “Veterinary Science for One Health” and its coordinator, Prof. HORIUCHI Motohiro (Laboratory of Veterinary Hygiene, Preventive Veterinary Medicine, Division of Veterinary Medicine, Faculty of Veterinary Medicine, HU). This program has provided me the opportunity to study and learn science and English without worrying about a student loan debt. I also thank the members of the Leading Program Office for their support with regards to my Ph.D. training.

I would like to thank Dr. MATSUNO Keita (Laboratory of Microbiology, Department of Disease Control, Faculty of Veterinary Medicine, HU), Dr. KAJIHARA Masahiro, Dr. MURAMATSU Mieko, Dr. NOYORI Osamu, Dr. KURODA Makoto, Dr. MARUYAMA Junki, Dr. NAO Naganori, Dr. FURUYAMA Wakako, Ms. MIYAMOTO Hiroko, Ms. SHIGENO Asako, Ms. MORI-KAJIHARA Akina (Division of Global epidemiology, CZC, HU) for their suggestions and frequent pep talks.

I would like to thank the staff at the CZC, especially Ms. ONUMA Aiko, for her assistance with my research activities, GE Healthcare Japan Corporation and SATO Shinichiro (Hokkaido WAKO) for their assistance with the establishment of the IN Cell Analyzer 2000 protocol, and Life Technologies Japan, Ltd. and Frontier Science co., Ltd. for their assistance with gene editing. I would also like to thank Dr. SASAKI Michihito (Division of Molecular Pathobiology, CZC, HU) for providing me the anti-LAMP1 antibody, and Dr. BEST Sonja (NIAID, NIH, RML) for providing me the pIFNβ-luc plasmid. I am grateful to HENSHOW Michael, EMANUELL Jackson, BARRYMORE Kim, and Editage (www.editage.jp) for helping me improve English.

I am forever grateful to my family, especially to my mother, for her understanding and patience for 30 years. I wish to especially thank my huge inspirations: Thouzer, Raoh, MAKUNOUCHI Ippo, KAMOGAWA Genji, TAKAMURA Mamoru, Zebra, Sakazuki (Akainu), Donquixote Doflamingo, Rockman (Megaman), Ultraman and its enemies, Kamen-rider and its enemies, SUGISHITA Ukyo, YAMI Sukehiro, Goku, Begeta, GeGeGe-no-Kitaro, and HAZAMA Kuroo. Their words and actions have often helped me regain my self-belief, remain calm and composed especially during stressful times, and come up with creative and ambitious ideas.

Finally, my research was funded by the Research Fellowship for Young Scientists from the Japan Society for the Promotion of Science (JSPS, 16J04404) and by the Gene Grant from the NIPPON Genetics Co, Ltd. Funding was also provided in part by the Intramural Research Program, NIAID, NIH; by the Japanese Initiative for Progress of Research on Infectious Disease for Global Epidemics (J-PRIDE, JP17fm0208101) from the Japan Agency for Medical Research and Development (AMED); and by the Science and Technology Research Partnership for Sustainable Development (SATREPS, 15JM0110005H0004).

Abstract in Japanese（和文要旨）

エボラウイルスおよびマールブルグウイルスは、フィロウイルス科に属し、ヒトを含む霊長類動物に重篤な出血熱を引き起こす人獣共通感染症病原体である。フィロウイルス科は進化系統学的に 3 属（エボラウイルス属、マールブルグウイルス属、キュエヴァウイルス属）に分類され、計 8 種のウイルス（エボラウイルス、ブンディブギョウイルス、タイフォレストウイルス、スーダンウイルス、レストンウイルス、マールブルグウイルス、ラブンウイルス、ヨビュウウイルス）が報告されている。エボラウイルス、ブンディブギョウイルス、スーダンウイルス、マールブルグウイルスによる出血熱は中央および西アフリカで散発的に発生し、近年、その頻度が増加傾向にあることから、公衆衛生上の注意が払われている。フィロウイルスは種々の動物種由来の細胞に感受性を示すことが報告されており、フィロウイルスが持つ蛋白質と相互作用する宿主側の因子も多数報告されている。しかし、その分子基盤については未だ不明な点が多い。本論文では、フィロウイルスの細胞侵入、転写・複製および免疫抑制機構に関わるウイルス蛋白質と宿主因子の相互作用に着目した。

フィロウイルスは、粒子表面糖蛋白質 GP を介して細胞表面に吸着し、細胞内小胞に取り込まれる。後期エンドソームへと移動した後、GP は酸性 pH 下で宿主プロテアーゼにより部分的に分解される。分解を受けレセプター結合領域が露出した GP は、同じ

く後期エンドソーム内に発現する NPC1 と結合する。この GP と NPC1 の相互作用がウイルスエンベロープとエンドソーム膜の融合の引き金となる。したがって、NPC1 はフィロウイルスの細胞侵入において必須の分子と考えられている。第一章では、この NPC1 の一塩基多型（SNP）に着目し、ヒト NPC1 の SNP がフィロウイルスの細胞侵入効率に与える影響を解析した。GP と相互作用する NPC1 領域の SNP を調べたところ、8 箇所のアミノ酸（419、420、424、425、427、500、502、508 番目）に計 10 個の SNP があることが分かった。これらの SNP がフィロウイルスの細胞侵入に与える影響を解析するために、先ず、NPC1 をノックアウトした Vero E6 細胞（Vero E6/NPC1-KO）を作製した。その後、レトロウイルスベクターを用いて、ヒト由来の野生型 NPC1 または各 SNP を導入した NPC1 遺伝子を Vero E6/NPC1-KO へ導入し、各々の NPC1 恒常発現細胞を作出した。各恒常発現細胞のフィロウイルスに対する感受性を、フィロウイルスの GP をもつシュードタイプウイルスおよび感染性エボラウイルスを用いて評価した。Vero E6/NPC1-KO では、シュードタイプウイルスおよび感染性エボラウイルスに対する感受性が失われる事を確認後、Vero E6/NPC1-KO にヒト由来の野生型 NPC1 を導入すると、再びそれらのウイルスの感染が成立することが分かった。計 10 個の SNP のうち、エボラウイルスでは 424 番目と 508 番目に SNP を有する細胞で、マールブルグウイルスでは 425 番目と 502 番目に SNP を有する細胞で、ウイルスの感染価が低くなる傾向が認められた。これらの結果は、NPC1 の SNP がフィロウイルス

に対するヒトの感受性に影響を与える可能性を示唆している。

膜融合によりウイルス蛋白質（NP、VP35、VP30、VP24 および L 蛋白質）とウイルスゲノムの複合体が細胞質内に放出されると、ウイルスゲノムの転写および複製が始まる。フィロウイルスの VP35 は宿主細胞における IFN-β 産生を抑制する事ならびにウイルスポリメラーゼコファクターとして転写や複製に関わる事が知られている。近年、この VP35 と高い相同性を有するアミノ酸配列をコードする領域（mlEFL35）がトビイロホオヒゲコウモリのゲノム内に発見された。コウモリは、フィロウイルスの自然宿主あるいはレゼルボアとして有力視されている動物であり、mlEFL35 はフィロウイルスの感染制御に関わる宿主因子を発現する可能性が推測されていた。第二章では、mlEFL35 の生物学的意義を考察することを目的として、mlEFL35 がコードする蛋白質（mlEFL35p）を培養細胞に発現させ、その機能解析を行った。エボラウイルスの VP35 と mlEFL35p のアミノ酸配列を詳細に比較したところ、多量体形成および IFN 応答抑制に必要な領域に高い相同性が見られたが、ポリメラーゼコファクター活性に重要なアミノ酸は保存されていなかった。mlEFL35p 発現プラスミドを HEK293T 細胞に導入したところ VP35 と同様に細胞質への局在が確認された。VP35 を共発現させた細胞を用いた免疫沈降法の結果から、mlEFL35p は多量体を形成し、エボラウイルスの VP35 とも相互作用することが示唆された。mlEFL35p を発現させた細胞では、VP35 発現と同様に、RIG-I、IPS-1 および TBK1 によるヒト IFN-β プロモーターの活性化が抑制さ

れた。次に、エボラウイルスのミニゲノムアッセイを用いて、mlEFL35p の発現がウイルスゲノムの転写・複製に与える影響を解析した結果、mlEFL35p は VP35 の機能を補完することはなく、mlEFL35p の過剰発現はウイルスゲノムからのレポーター遺伝子の発現を微弱ながら抑制する事が分かった。これらの結果は、mlEFL35p はフィロウイルスの VP35 同様に IFN 応答阻害活性を有する一方で、ウイルスポリメラーゼコファクターとしての機能は持たないことを示している。

本論文では、同一宿主種内に見られる遺伝子多型がフィロウイルスの細胞指向性に影響を与えうることを示した。GP と NPC1 の相互作用は、宿主特異性・宿主域決定に関与するだけでなく、同じ動物種内の個体レベルの感受性の違いにも関与していると考えられる。今後、ヒトの遺伝的多様性がより詳細に明らかになれば、地域間あるいは人種間等の SNP 分布と流行地域あるいは感受性との間に関連を見出すことも可能かもしれない。また、本論文ではコウモリのゲノムに見つかったフィロウイルス様遺伝子がコードする宿主蛋白質が、ウイルス蛋白質と似た性質を有することも示した。しかし、生体内での mlEFL35/mlEFL35p の挙動や宿主の免疫反応との関連など不明な点は数多く残されている。今後は、個体間あるいは動物間におけるフィロウイルス様遺伝子の存在・発現様式の違いおよびそれが生体に与える影響、特にフィロウイルスに対する感受性との関連性について明らかにする必要がある。

ウイルス感染による宿主の病態は、ウイルス側の因子および宿主側の因子の相互作用

が蓄積した結果であり、その相互作用の全容解明はウイルスの病原性と宿主域を理解するために重要である。また、病原性発現に関わる要因が明らかになれば、それを標的とした新たな創薬開発への展開が期待される。本論文で示したアプローチと概念は、他のウイルス感染症にも応用可能であり、今後、より広汎かつ詳細な基礎研究によって、様々なウイルス感染症の制御に貢献することを期待したい。

References

1) Antony JM, Ellestad KK, Hammond R, Imaizumi K, Mallet F, Warren KG, Power C. The human endogenous retrovirus envelope glycoprotein, syncytin-1, regulates neuroinflammation and its receptor expression in multiple sclerosis: a role for endoplasmic reticulum chaperones in astrocytes. J Immunol 179, 1210-1224, 2007.

2) Aswad A, Katzourakis A. Paleovirology and virally derived immunity. Trends Ecol Evol 27, 627-636, 2012.

3) Bannert N, Kurth R. Retroelements and the human genome: new perspectives on an old relation. Proc Natl Acad Sci U S A 101 Suppl 2, 14572-14579, 2004.

4) Baron RC, McCormick JB, Zubeir OA. Ebola virus disease in southern Sudan: hospital dissemination and intrafamilial spread. Bull World Health Organ 61, 997-1003, 1983.

5) Basler CF, Amarasinghe GK. Evasion of interferon responses by Ebola and Marburg viruses. J Interferon Cytokine Res 29, 511-520, 2009.

6) Belyi VA, Levine AJ, Skalka AM. Unexpected inheritance: multiple integrations of ancient bornavirus and ebolavirus/marburgvirus sequences in vertebrate genomes. PLoS Pathog 6, e1001030, 2010.

7) Blaise S, de Parseval N, Benit L, Heidmann T. Genomewide screening for fusogenic human endogenous retrovirus envelopes identifies syncytin 2, a gene conserved on primate evolution. Proc Natl Acad Sci U S A 100, 13013-13018, 2003.

8) Cantoni D, Hamlet A, Michaelis M, Wass MN, Rossman JS. Risks Posed by Reston, the Forgotten Ebolavirus. mSphere 1, 2016.

9) Cardenas WB, Loo YM, Gale M, Jr., Hartman AL, Kimberlin CR, Martinez-Sobrido L, Saphire EO, Basler CF. Ebola virus VP35 protein binds double-stranded RNA and inhibits alpha/beta interferon production induced by RIG-I signaling. J Virol 80, 5168-5178, 2006.

10) Carette JE, Raaben M, Wong AC, Herbert AS, Obernosterer G, Mulherkar N, Kuehne AI, Kranzusch PJ, Griffin AM, Ruthel G, Dal Cin P, Dye JM, Whelan SP, Chandran K, Brummelkamp TR. Ebola virus entry requires the cholesterol transporter Niemann-Pick C1. Nature 477, 340-343, 2011.

11) Chan SY, Speck RF, Ma MC, Goldsmith MA. Distinct mechanisms of entry by envelope glycoproteins of Marburg and Ebola (Zaire) viruses. J Virol 74, 4933-4937, 2000.

12) Chandran K, Sullivan NJ, Felbor U, Whelan SP, Cunningham JM. Endosomal proteolysis of the Ebola virus glycoprotein is necessary for infection. Science 308, 1643-1645, 2005.

13) Changula K, Kajihara M, Mweene AS, Takada A. Ebola and Marburg virus diseases in Africa: increased risk of outbreaks in previously unaffected areas? Microbiol Immunol 58, 483-491, 2014.

14) Changula K, Yoshida R, Noyori O, Marzi A, Miyamoto H, Ishijima M, Yokoyama A, Kajihara M, Feldmann H, Mweene AS, Takada A. Mapping of conserved and species-specific antibody epitopes on the Ebola virus nucleoprotein. Virus Res 176, 83-90, 2013.

15) Cote M, Misasi J, Ren T, Bruchez A, Lee K, Filone CM, Hensley L, Li Q, Ory D, Chandran K, Cunningham J. Small molecule inhibitors reveal Niemann-Pick C1 is essential for Ebola virus infection. Nature 477, 344-348, 2011.

16) Davies JP, Ioannou YA. Topological analysis of Niemann-Pick C1 protein reveals that the membrane orientation of the putative sterol-sensing domain is identical to those of 3-hydroxy-3-methylglutaryl-CoA reductase and sterol regulatory element binding protein cleavage-activating protein. J Biol Chem 275, 24367-24374, 2000.

17) Dayhoff M, Schwartz R, Orcutt B. A model of evolutionary change in proteins. Atlas of protein sequence and structure, 345-352, 1978.

18) Dean NE, Halloran ME, Yang Y, Longini IM. Transmissibility and Pathogenicity of Ebola Virus: A Systematic Review and Meta-analysis of Household Secondary Attack Rate and Asymptomatic Infection. Clin Infect Dis 62, 1277-1286, 2016.

19) Dupressoir A, Marceau G, Vernochet C, Benit L, Kanellopoulos C, Sapin V, Heidmann T. Syncytin-A and syncytin-B, two fusogenic placenta-specific murine envelope genes of retroviral origin conserved in Muridae. Proc Natl Acad Sci U S A 102, 725-730, 2005.

20) Ebihara H, Takada A, Kobasa D, Jones S, Neumann G, Theriault S, Bray M, Feldmann H, Kawaoka Y. Molecular determinants of Ebola virus virulence in mice. PLoS Pathog 2, e73, 2006.

21) Ebihara H, Theriault S, Neumann G, Alimonti JB, Geisbert JB, Hensley LE, Groseth A, Jones SM, Geisbert TW, Kawaoka Y, Feldmann H. In vitro and in vivo characterization of recombinant Ebola viruses expressing enhanced green fluorescent protein. J Infect Dis 196 Suppl 2, S313-322, 2007.

22) Ebihara H, Yoshimatsu K, Ogino M, Araki K, Ami Y, Kariwa H, Takashima I, Li D, Arikawa J. Pathogenicity of Hantaan virus in newborn mice: genetic reassortant study demonstrating that a single amino acid change in glycoprotein G1 is related to virulence. J Virol 74, 9245-9255, 2000.

23) Elliott LH, Kiley MP, McCormick JB. Descriptive analysis of Ebola virus proteins. Virology 147, 169-176, 1985.

24) Fujino K, Horie M, Honda T, Merriman DK, Tomonaga K. Inhibition of Borna disease virus replication by an endogenous bornavirus-like element in the ground squirrel genome. Proc Natl Acad Sci U S A 111, 13175-13180, 2014.

25) Furuyama W, Miyamoto H, Yoshida R, Takada A. Quantification of Filovirus Glycoprotein-Specific Antibodies. Methods Mol Biol 1628, 309-320, 2017.

26) Gack MU, Albrecht RA, Urano T, Inn KS, Huang IC, Carnero E, Farzan M, Inoue S, Jung JU, Garcia-Sastre A. Influenza A virus NS1 targets the ubiquitin ligase TRIM25 to evade recognition by the host viral RNA sensor RIG-I. Cell Host Microbe 5, 439-449, 2009.

27) Goldstein T, Anthony SJ, Gbakima A, Bird BH, Bangura J, Tremeau-Bravard A, Belaganahalli MN, Wells HL, Dhanota JK, Liang E, Grodus M, Jangra RK, DeJesus VA, Lasso G, Smith BR, Jambai A, Kamara BO, Kamara S, Bangura W, Monagin C, Shapira S, Johnson CK, Saylors K, Rubin EM, Chandran K, Lipkin WI, Mazet JAK. The discovery of Bombali virus adds further support for bats as hosts of ebolaviruses. Nat Microbiol 3, 1084-1089, 2018.

28) Gong X, Qian H, Zhou X, Wu J, Wan T, Cao P, Huang W, Zhao X, Wang X, Wang P, Shi Y, Gao GF, Zhou Q, Yan N. Structural Insights into the Niemann-Pick C1 (NPC1)-Mediated Cholesterol Transfer and Ebola Infection. Cell 165, 1467-1478, 2016.

29) Guito JC, Albarino CG, Chakrabarti AK, Towner JS. Novel activities by ebolavirus and marburgvirus interferon antagonists revealed using a standardized in vitro reporter system. Virology 501, 147-165, 2017.

30) Harcourt BH, Sanchez A, Offermann MK. Ebola virus inhibits induction of genes by double-stranded RNA in endothelial cells. Virology 252, 179-188, 1998.

31) Hartman AL, Bird BH, Towner JS, Antoniadou ZA, Zaki SR, Nichol ST. Inhibition of IRF-3 activation by VP35 is critical for the high level of virulence of Ebola virus. J Virol 82, 2699-2704, 2008.

32) Hartman AL, Towner JS, Nichol ST. A C-terminal basic amino acid motif of Zaire ebolavirus VP35 is essential for type I interferon antagonism and displays high identity with the RNA-binding domain of another interferon antagonist, the NS1 protein of influenza A virus. Virology 328, 177-184, 2004.

33) He P, Sun L, Zhu D, Zhang H, Zhang L, Guo Y, Liu S, Zhou J, Xu X, Xie P. Knock-Down of Endogenous Bornavirus-Like Nucleoprotein 1 Inhibits Cell Growth and Induces Apoptosis in Human Oligodendroglia Cells. Int J Mol Sci 17, 435, 2016.

34) Hill-Batorski L, Halfmann P, Marzi A, Lopes TJ, Neumann G, Feldmann H, Kawaoka Y. Loss of Interleukin 1 Receptor Antagonist Enhances Susceptibility to Ebola Virus Infection. J Infect Dis 212 Suppl 2, S329-335, 2015.

35) Hofmann-Winkler H, Kaup F, Pohlmann S. Host cell factors in filovirus entry: novel players, new insights. Viruses 4, 3336-3362, 2012.

36) Horie M, Honda T, Suzuki Y, Kobayashi Y, Daito T, Oshida T, Ikuta K, Jern P, Gojobori T, Coffin JM, Tomonaga K. Endogenous non-retroviral RNA virus elements in mammalian genomes. Nature 463, 84-87, 2010.

37) Kajihara M, Nakayama E, Marzi A, Igarashi M, Feldmann H, Takada A. Novel mutations in

Marburg virus glycoprotein associated with viral evasion from antibody mediated immune pressure. J Gen Virol 94, 876-883, 2013.

38) Kajihara M, Takada A. Host Cell Factors Involved in Filovirus Infection. Current Tropical Medicine Reports 2, 30-40, 2015.

39) Kash JC, Muhlberger E, Carter V, Grosch M, Perwitasari O, Proll SC, Thomas MJ, Weber F, Klenk HD, Katze MG. Global suppression of the host antiviral response by Ebola- and Marburgviruses: increased antagonism of the type I interferon response is associated with enhanced virulence. J Virol 80, 3009-3020, 2006.

40) Katoh K, Misawa K, Kuma K, Miyata T. MAFFT: a novel method for rapid multiple sequence alignment based on fast Fourier transform. Nucleic Acids Res 30, 3059-3066, 2002.

41) Kawai T, Takahashi K, Sato S, Coban C, Kumar H, Kato H, Ishii KJ, Takeuchi O, Akira S. IPS-1, an adaptor triggering RIG-I- and Mda5-mediated type I interferon induction. Nat Immunol 6, 981-988, 2005.

42) Kemenesi G, Kurucz K, Dallos B, Zana B, Foldes F, Boldogh S, Gorfol T, Carroll MW, Jakab F. Re-emergence of Lloviu virus in Miniopterus schreibersii bats, Hungary, 2016. Emerg Microbes Infect 7, 66, 2018.

43) Kirchdoerfer RN, Abelson DM, Li S, Wood MR, Saphire EO. Assembly of the Ebola Virus Nucleoprotein from a Chaperoned VP35 Complex. Cell Rep 12, 140-149, 2015.

44) Kitamura T, Koshino Y, Shibata F, Oki T, Nakajima H, Nosaka T, Kumagai H. Retrovirus-mediated gene transfer and expression cloning: powerful tools in functional genomics. Exp Hematol 31, 1007-1014, 2003.

45) Kuhn JH. Guide to the Correct Use of Filoviral Nomenclature. Curr Top Microbiol Immunol 411, 447-460, 2017.

46) Kuroda M, Fujikura D, Nanbo A, Marzi A, Noyori O, Kajihara M, Maruyama J, Matsuno K, Miyamoto H, Yoshida R, Feldmann H, Takada A. Interaction between TIM-1 and NPC1 Is Important for Cellular Entry of Ebola Virus. J Virol 89, 6481-6493, 2015.

47) Leroy EM, Kumulungui B, Pourrut X, Rouquet P, Hassanin A, Yaba P, Delicat A, Paweska JT, Gonzalez JP, Swanepoel R. Fruit bats as reservoirs of Ebola virus. Nature 438, 575-576, 2005.

48) Leung DW, Borek D, Luthra P, Binning JM, Anantpadma M, Liu G, Harvey IB, Su Z, Endlich-Frazier A, Pan J, Shabman RS, Chiu W, Davey RA, Otwinowski Z, Basler CF, Amarasinghe GK. An Intrinsically Disordered Peptide from Ebola Virus VP35 Controls Viral RNA Synthesis by Modulating Nucleoprotein-RNA Interactions. Cell Rep 11, 376-389, 2015.

49) Leung DW, Ginder ND, Fulton DB, Nix J, Basler CF, Honzatko RB, Amarasinghe GK. Structure of the Ebola VP35 interferon inhibitory domain. Proc Natl Acad Sci U S A 106, 411-416, 2009.

50) Leung DW, Prins KC, Borek DM, Farahbakhsh M, Tufariello JM, Ramanan P, Nix JC,

Helgeson LA, Otwinowski Z, Honzatko RB, Basler CF, Amarasinghe GK. Structural basis for dsRNA recognition and interferon antagonism by Ebola VP35. Nat Struct Mol Biol 17, 165-172, 2010.

51) Leung DW, Shabman RS, Farahbakhsh M, Prins KC, Borek DM, Wang T, Muhlberger E, Basler CF, Amarasinghe GK. Structural and functional characterization of Reston Ebola virus VP35 interferon inhibitory domain. J Mol Biol 399, 347-357, 2010.

52) Liang X, Potter J, Kumar S, Zou Y, Quintanilla R, Sridharan M, Carte J, Chen W, Roark N, Ranganathan S, Ravinder N, Chesnut JD. Rapid and highly efficient mammalian cell engineering via Cas9 protein transfection. J Biotechnol 208, 44-53, 2015.

53) Liu B, Dong S, Li G, Wang W, Liu X, Wang Y, Yang C, Rao Z, Guo Y. Structural Insight into Nucleoprotein Conformation Change Chaperoned by VP35 Peptide in Marburg Virus. J Virol 91, 2017.

54) Liu R, Paxton WA, Choe S, Ceradini D, Martin SR, Horuk R, MacDonald ME, Stuhlmann H, Koup RA, Landau NR. Homozygous defect in HIV-1 coreceptor accounts for resistance of some multiply-exposed individuals to HIV-1 infection. Cell 86, 367-377, 1996.

55) Luthra P, Jordan DS, Leung DW, Amarasinghe GK, Basler CF. Ebola virus VP35 interaction with dynein LC8 regulates viral RNA synthesis. J Virol 89, 5148-5153, 2015.

56) Luthra P, Ramanan P, Mire CE, Weisend C, Tsuda Y, Yen B, Liu G, Leung DW, Geisbert TW, Ebihara H, Amarasinghe GK, Basler CF. Mutual antagonism between the Ebola virus VP35 protein and the RIG-I activator PACT determines infection outcome. Cell Host Microbe 14, 74-84, 2013.

57) Machnik G, Skudrzyk E, Buldak L, Labuzek K, Ruczynski J, Alenowicz M, Rekowski P, Nowak PJ, Okopien B. A Novel, Highly Selective RT-QPCR Method for Quantification of MSRV Using PNA Clamping Syncytin-1 (ERVWE1). Mol Biotechnol 57, 801-813, 2015.

58) Mameli G, Astone V, Arru G, Marconi S, Lovato L, Serra C, Sotgiu S, Bonetti B, Dolei A. Brains and peripheral blood mononuclear cells of multiple sclerosis (MS) patients hyperexpress MS-associated retrovirus/HERV-W endogenous retrovirus, but not Human herpesvirus 6. J Gen Virol 88, 264-274, 2007.

59) Maruyama J, Miyamoto H, Kajihara M, Ogawa H, Maeda K, Sakoda Y, Yoshida R, Takada A. Characterization of the envelope glycoprotein of a novel filovirus, Lloviu virus. J Virol 88, 99-109, 2014.

60) Mi S, Lee X, Li X, Veldman GM, Finnerty H, Racie L, LaVallie E, Tang XY, Edouard P, Howes S, Keith JC, Jr., McCoy JM. Syncytin is a captive retroviral envelope protein involved in human placental morphogenesis. Nature 403, 785-789, 2000.

61) Miller EH, Obernosterer G, Raaben M, Herbert AS, Deffieu MS, Krishnan A, Ndungo E, Sandesara RG, Carette JE, Kuehne AI, Ruthel G, Pfeffer SR, Dye JM, Whelan SP,

Brummelkamp TR, Chandran K. Ebola virus entry requires the host-programmed recognition of an intracellular receptor. EMBO J 31, 1947-1960, 2012.

62) Misasi J, Chandran K, Yang JY, Considine B, Filone CM, Cote M, Sullivan N, Fabozzi G, Hensley L, Cunningham J. Filoviruses require endosomal cysteine proteases for entry but exhibit distinct protease preferences. J Virol 86, 3284-3292, 2012.

63) Moller P, Pariente N, Klenk HD, Becker S. Homo-oligomerization of Marburgvirus VP35 is essential for its function in replication and transcription. J Virol 79, 14876-14886, 2005.

64) Muhlberger E, Weik M, Volchkov VE, Klenk HD, Becker S. Comparison of the transcription and replication strategies of marburg virus and Ebola virus by using artificial replication systems. J Virol 73, 2333-2342, 1999.

65) Myers KN, Barone G, Ganesh A, Staples CJ, Howard AE, Beveridge RD, Maslen S, Skehel JM, Collis SJ. The bornavirus-derived human protein EBLN1 promotes efficient cell cycle transit, microtubule organisation and genome stability. Sci Rep 6, 35548, 2016.

66) Naito Y, Hino K, Bono H, Ui-Tei K. CRISPRdirect: software for designing CRISPR/Cas guide RNA with reduced off-target sites. Bioinformatics 31, 1120-1123, 2015.

67) Nanbo A, Imai M, Watanabe S, Noda T, Takahashi K, Neumann G, Halfmann P, Kawaoka Y. Ebolavirus is internalized into host cells via macropinocytosis in a viral glycoprotein-dependent manner. PLoS Pathog 6, e1001121, 2010.

68) Ndungo E, Herbert AS, Raaben M, Obernosterer G, Biswas R, Miller EH, Wirchnianski AS, Carette JE, Brummelkamp TR, Whelan SP, Dye JM, Chandran K. A Single Residue in Ebola Virus Receptor NPC1 Influences Cellular Host Range in Reptiles. mSphere 1, 2016.

69) Negredo A, Palacios G, Vazquez-Moron S, Gonzalez F, Dopazo H, Molero F, Juste J, Quetglas J, Savji N, de la Cruz Martinez M, Herrera JE, Pizarro M, Hutchison SK, Echevarria JE, Lipkin WI, Tenorio A. Discovery of an ebolavirus-like filovirus in europe. PLoS Pathog 7, e1002304, 2011.

70) Ng M, Ndungo E, Kaczmarek ME, Herbert AS, Binger T, Kuehne AI, Jangra RK, Hawkins JA, Gifford RJ, Biswas R, Demogines A, James RM, Yu M, Brummelkamp TR, Drosten C, Wang LF, Kuhn JH, Muller MA, Dye JM, Sawyer SL, Chandran K. Filovirus receptor NPC1 contributes to species-specific patterns of ebolavirus susceptibility in bats. Elife 4, 2015.

71) Niwa H, Yamamura K, Miyazaki J. Efficient selection for high-expression transfectants with a novel eukaryotic vector. Gene 108, 193-199, 1991.

72) O'Brien SJ, Moore JP. The effect of genetic variation in chemokines and their receptors on HIV transmission and progression to AIDS. Immunol Rev 177, 99-111, 2000.

73) Ogawa H, Miyamoto H, Nakayama E, Yoshida R, Nakamura I, Sawa H, Ishii A, Thomas Y, Nakagawa E, Matsuno K, Kajihara M, Maruyama J, Nao N, Muramatsu M, Kuroda M, Simulundu E, Changula K, Hang'ombe B, Namangala B, Nambota A, Katampi J, Igarashi M,

Ito K, Feldmann H, Sugimoto C, Moonga L, Mweene A, Takada A. Seroepidemiological Prevalence of Multiple Species of Filoviruses in Fruit Bats (Eidolon helvum) Migrating in Africa. J Infect Dis 212 Suppl 2, S101-108, 2015.

74) Pereyra F, Addo MM, Kaufmann DE, Liu Y, Miura T, Rathod A, Baker B, Trocha A, Rosenberg R, Mackey E, Ueda P, Lu Z, Cohen D, Wrin T, Petropoulos CJ, Rosenberg ES, Walker BD. Genetic and immunologic heterogeneity among persons who control HIV infection in the absence of therapy. J Infect Dis 197, 563-571, 2008.

75) Pourrut X, Souris M, Towner JS, Rollin PE, Nichol ST, Gonzalez JP, Leroy E. Large serological survey showing cocirculation of Ebola and Marburg viruses in Gabonese bat populations, and a high seroprevalence of both viruses in Rousettus aegyptiacus. BMC Infect Dis 9, 159, 2009.

76) Prins KC, Binning JM, Shabman RS, Leung DW, Amarasinghe GK, Basler CF. Basic residues within the ebolavirus VP35 protein are required for its viral polymerase cofactor function. J Virol 84, 10581-10591, 2010.

77) Prins KC, Cardenas WB, Basler CF. Ebola virus protein VP35 impairs the function of interferon regulatory factor-activating kinases IKKepsilon and TBK-1. J Virol 83, 3069-3077, 2009.

78) Rasmussen AL, Okumura A, Ferris MT, Green R, Feldmann F, Kelly SM, Scott DP, Safronetz D, Haddock E, LaCasse R, Thomas MJ, Sova P, Carter VS, Weiss JM, Miller DR, Shaw GD, Korth MJ, Heise MT, Baric RS, de Villena FP, Feldmann H, Katze MG. Host genetic diversity enables Ebola hemorrhagic fever pathogenesis and resistance. Science 346, 987-991, 2014.

79) Reid SP, Cardenas WB, Basler CF. Homo-oligomerization facilitates the interferon-antagonist activity of the ebolavirus VP35 protein. Virology 341, 179-189, 2005.

80) Rolland A, Jouvin-Marche E, Viret C, Faure M, Perron H, Marche PN. The envelope protein of a human endogenous retrovirus-W family activates innate immunity through CD14/TLR4 and promotes Th1-like responses. J Immunol 176, 7636-7644, 2006.

81) Saeed MF, Kolokoltsov AA, Albrecht T, Davey RA. Cellular entry of ebola virus involves uptake by a macropinocytosis-like mechanism and subsequent trafficking through early and late endosomes. PLoS Pathog 6, e1001110, 2010.

82) Samson M, Libert F, Doranz BJ, Rucker J, Liesnard C, Farber CM, Saragosti S, Lapoumeroulie C, Cognaux J, Forceille C, Muyldermans G, Verhofstede C, Burtonboy G, Georges M, Imai T, Rana S, Yi Y, Smyth RJ, Collman RG, Doms RW, Vassart G, Parmentier M. Resistance to HIV-1 infection in caucasian individuals bearing mutant alleles of the CCR-5 chemokine receptor gene. Nature 382, 722-725, 1996.

83) Shiwani HA, Pharithi RB, Khan B, Egom CB, Kruzliak P, Maher V, Egom EE. An update on the 2014 Ebola outbreak in Western Africa. Asian Pac J Trop Med 10, 6-10, 2017.

84) Sofuku K, Parrish NF, Honda T, Tomonaga K. Transcription Profiling Demonstrates Epigenetic Control of Non-retroviral RNA Virus-Derived Elements in the Human Genome. Cell Rep 12, 1548-1554, 2015.

85) Spiropoulou CF, Ranjan P, Pearce MB, Sealy TK, Albarino CG, Gangappa S, Fujita T, Rollin PE, Nichol ST, Ksiazek TG, Sambhara S. RIG-I activation inhibits ebolavirus replication. Virology 392, 11-15, 2009.

86) Stoye JP. Studies of endogenous retroviruses reveal a continuing evolutionary saga. Nat Rev Microbiol 10, 395-406, 2012.

87) Swanepoel R, Leman PA, Burt FJ, Zachariades NA, Braack LE, Ksiazek TG, Rollin PE, Zaki SR, Peters CJ. Experimental inoculation of plants and animals with Ebola virus. Emerg Infect Dis 2, 321-325, 1996.

88) Takada A. Filovirus tropism: cellular molecules for viral entry. Front Microbiol 3, 34, 2012.

89) Takada A, Feldmann H, Stroeher U, Bray M, Watanabe S, Ito H, McGregor M, Kawaoka Y. Identification of protective epitopes on ebola virus glycoprotein at the single amino acid level by using recombinant vesicular stomatitis viruses. J Virol 77, 1069-1074, 2003.

90) Takada A, Robison C, Goto H, Sanchez A, Murti KG, Whitt MA, Kawaoka Y. A system for functional analysis of Ebola virus glycoprotein. Proc Natl Acad Sci U S A 94, 14764-14769, 1997.

91) Talon J, Horvath CM, Polley R, Basler CF, Muster T, Palese P, Garcia-Sastre A. Activation of interferon regulatory factor 3 is inhibited by the influenza A virus NS1 protein. J Virol 74, 7989-7996, 2000.

92) Taylor DJ, Ballinger MJ, Zhan JJ, Hanzly LE, Bruenn JA. Evidence that ebolaviruses and cuevaviruses have been diverging from marburgviruses since the Miocene. PeerJ 2, e556, 2014.

93) Taylor DJ, Dittmar K, Ballinger MJ, Bruenn JA. Evolutionary maintenance of filovirus-like genes in bat genomes. BMC Evol Biol 11, 336, 2011.

94) Taylor DJ, Leach RW, Bruenn J. Filoviruses are ancient and integrated into mammalian genomes. BMC Evol Biol 10, 193, 2010.

95) Team RC. R: A language and environment for statistical computing, 2013.

96) Trunschke M, Conrad D, Enterlein S, Olejnik J, Brauburger K, Muhlberger E. The L-VP35 and L-L interaction domains reside in the amino terminus of the Ebola virus L protein and are potential targets for antivirals. Virology 441, 135-145, 2013.

97) Wang H, Shi Y, Song J, Qi J, Lu G, Yan J, Gao GF. Ebola Viral Glycoprotein Bound to Its Endosomal Receptor Niemann-Pick C1. Cell 164, 258-268, 2016.

98) Watanabe S, Noda T, Halfmann P, Jasenosky L, Kawaoka Y. Ebola virus (EBOV) VP24 inhibits transcription and replication of the EBOV genome. J Infect Dis 196 Suppl 2, S284-

290, 2007.

99) Yu X, Liang X, Xie H, Kumar S, Ravinder N, Potter J, de Mollerat du Jeu X, Chesnut JD. Improved delivery of Cas9 protein/gRNA complexes using lipofectamine CRISPRMAX. Biotechnol Lett 38, 919-929, 2016.

100) Yuan J, Zhang Y, Li J, Zhang Y, Wang LF, Shi Z. Serological evidence of ebolavirus infection in bats, China. Virol J 9, 236, 2012.